NAVAL POSTGRADUATE SCHOOL

MONTEREY, CALIFORNIA

THESIS

DESIGN AND IMPLEMENTATION OF A DSP-BASED CONTROL INTERFACE UNIT (CIU)

by

Andreas Kavousanos-Kavousanakis

March 2004

Thesis Advisor:	Xiaoping Yun
Second Reader:	David C. Jenn

Approved for public release; distribution is unlimited

THIS PAGE INTENTIONALLY LEFT BLANK

REPORT DOCUMENTATION PAGE			Form Approved OMB No. 0704-0188
Public reporting burden for this collection of information is estimated to average 1 hour per response, including the time for reviewing instruction, searching existing data sources, gathering and maintaining the data needed, and completing and reviewing the collection of information. Send comments regarding this burden estimate or any other aspect of this collection of information, including suggestions for reducing this burden, to Washington headquarters Services, Directorate for Information Operations and Reports, 1215 Jefferson Davis Highway, Suite 1204, Arlington, VA 22202-4302, and to the Office of Management and Budget, Paperwork Reduction Project (0704-0188) Washington DC 20503.			
1. AGENCY USE ONLY *(Leave blank)*	**2. REPORT DATE** March 2004	**3. REPORT TYPE AND DATES COVERED** Master's Thesis	
4. TITLE AND SUBTITLE: Design and Implementation of a DSP-Based Control Interface Unit (CIU)		**5. FUNDING NUMBERS**	
6. AUTHOR(S) Andreas Kavousanos-Kavousanakis			
7. PERFORMING ORGANIZATION NAME(S) AND ADDRESS(ES) Naval Postgraduate School Monterey, CA 93943-5000		**8. PERFORMING ORGANIZATION REPORT NUMBER**	
9. SPONSORING / MONITORING AGENCY NAME(S) AND ADDRESS(ES) U.S. Army Research Office (ARO) U.S. Navy Modeling and Simulation Office (N6M)		**10. SPONSORING / MONITORING AGENCY REPORT NUMBER**	
11. SUPPLEMENTARY NOTES The views expressed in this thesis are those of the author and do not reflect the official policy or position of the Department of Defense or the U.S. Government.			
12a. DISTRIBUTION / AVAILABILITY STATEMENT Approved for public release; distribution is unlimited.		**12b. DISTRIBUTION CODE**	

13. ABSTRACT (maximum 200 words)

This research involves the development of a human-body motion tracking system constructed with the use of commercial off-the-shelf (COTS) components. The main component of the system investigated in this thesis is the Control Interface Unit (CIU). The CIU is a component designed to receive data from the magnetic, angular rate, and gravity (MARG) sensors and prepare them to be transmitted through a wireless configuration. A simple and effective algorithm is used to filter the sensor data without singularities, providing the measured attitude in the quaternion form for each human limb. Initial calibration of the MARG sensors is also performed with the use of linear calibrating algorithms. The testing and evaluation of the whole system is performed by MATLAB® and SIMULINK® simulations, and by the real-time visualization using a human avatar designed with the X3D graphics specifications.

Through this research, it is discovered that the MARG sensors had to be redesigned to overcome an erratum on the Honeywell magnetometer HMC1051Z data sheet. With the redesigned MARG sensors, the testing results showed that the CIU was performing extremely well. The overall motion tracking system is capable of tracking human body limb motions in real time.

14. SUBJECT TERMS MARG III Sensor, Control Interface Unit (CIU), One-,Three-, Sixteen-Channel CIU, Avatar, Virtual Environment, Virtual Training, Immersion, Honeywell, Analog Devices, Texas Instruments, Microcontroller, Micromachined Sensor, X3D, Java, Xilinx, RS232, Wireless Communication, WiSER 2400.			**15. NUMBER OF PAGES** 86
			16. PRICE CODE
17. SECURITY CLASSIFICATION OF REPORT Unclassified	**18. SECURITY CLASSIFICATION OF THIS PAGE** Unclassified	**19. SECURITY CLASSIFICATION OF ABSTRACT** Unclassified	**20. LIMITATION OF ABSTRACT** UL

NSN 7540-01-280-5500

Standard Form 298 (Rev. 2-89)
Prescribed by ANSI Std. 239-18

THIS PAGE INTENTIONALLY LEFT BLANK

Approved for Public Release; Distribution is Unlimited

DESIGN AND IMPLEMENTATION OF A DSP-BASED CONTROL INTERFACE UNIT (CIU)

Andreas Kavousanos-Kavousanakis
Lieutenant Junior Grade, Hellenic Navy
B.S. in Naval Science, Hellenic Naval Academy, 1997
B.S. Equivalency in Electrical Engineering, Naval Postgraduate School, 2002

Submitted in partial fulfillment of the
requirements for the degree of

MASTER OF SCIENCE IN ELECTRICAL ENGINEERING
and
MASTER OF SCIENCE IN SYSTEMS ENGINEERING

from the

NAVAL POSTGRADUATE SCHOOL
March 2004

Author: Andreas Kavousanos-Kavousanakis

Approved by: Xiaoping Yun
Thesis Advisor

David C. Jenn
Second Reader

John P. Powers
Chairman, Department of Electrical and Computer Engineering

Dan C. Boger
Chairman, Department of Information Science

THIS PAGE INTENTIONALLY LEFT BLANK

ABSTRACT

This research involves the development of a human-body motion tracking system constructed with the use of commercial off-the-shelf (COTS) components. The main component of the system investigated in this thesis is the Control Interface Unit (CIU). The CIU is a component designed to receive data from the magnetic, angular rate, and gravity (MARG) sensors and prepare them to be transmitted through a wireless configuration. A simple and effective algorithm is used to filter the sensor data without singularities, providing the measured attitude in the quaternion form for each human limb. Initial calibration of the MARG sensors is also performed with the use of linear calibrating algorithms. The testing and evaluation of the whole system is performed by MATLAB® and SIMULINK® simulations, and by the real-time visualization using a human avatar designed with the X3D graphics specifications.

Through this research, it is discovered that the MARG sensors had to be redesigned to overcome an erratum on the Honeywell magnetometer HMC1051Z data sheet. With the redesigned MARG sensors, the testing results showed that the CIU was performing extremely well. The overall motion tracking system is capable of tracking human body limb motions in real time.

THIS PAGE INTENTIONALLY LEFT BLANK

TABLE OF CONTENTS

LIST OF FIGURES

LIST OF TABLES

THIS PAGE INTENTIONALLY LEFT BLANK

ACKNOWLEDGMENTS

Funding for the project was provided by the U.S. Army Research Office (ARO) and the U.S. Navy Modeling and Simulation Office (N6M). Without their support, we would not have had the necessary means to fulfill our goals, and this research would have never been completed.

I strongly feel that I owe everything I have accomplished in my life to my parents Georgios Kavousanos-Kavousanakis and Aliki Kavousanou-Kavousanaki. I would like to thank them for their constant guidance and support through my whole life. It was their endless love, care, and encouragement that enabled me to overcome any obstacles that I ever encountered.

It was Alexander the Great (356-323 BC) who said about his Teacher Aristotle that: *"I am indebted to my Parents for Living, but to my Teacher for Living Well"*. With this quote in mind, I would like to express my gratitude to my teacher and thesis advisor Professor Xiaoping Yun for his help and tireless support during the difficulties that I came across in my research. His brilliance guided me all the time to pursuit the appropriate paths in order to fulfill my ultimate goal: the creation of a unique motion tracking system.

I have to admit that the hardest part of my thesis was to have everything achieved, written down in a foreign language to me, and in such way that anybody would be able to understand. Even though Dr. Yun's native language is Chinese, I was completely amazed by the wealth of his knowledge in English.

I would like to thank Professor Robert G. Hutchins for passing me large fragments of his knowledge in the topic of quaternions, which is a topic extremely important to my research.

I would also like to thank James Calusdian for all his help in the lab. He was extremely helpful at the times an instrument and tool expert was needed.

My brothers Kostas and Christos, even though so far from me, helped me through many personal difficulties. Thank you for being there for me.

The two years I spent in Monterey studying for my degrees would have been totally different without Bridget Bevin. Bridget is the one who showed me what it is really like to live in the United States and she *immersed* me in a world that I wouldn't have understood otherwise. Thank you for being there for me at all times.

Many thanks to Faruk Yildiz for the hours and the combined effort we made together in order to complete our research. Faruk, our efforts finally paid off.

I would also like to thank Ron Russell for his meticulous and speedy editing of this thesis. His efficient work was extremely helpful to me.

Finally, I would like to thank Doug McKinney for putting up with me and my whining, over our endless phone and email conversations. Thank you for trusting my recommendations about the MARG III sensors.

«Εἰς τούς Γονεῖς μου χρεωστῶ τό Ζῆν, εἰς τόν Διδάσκαλό μου τό Εὖ Ζῆν»
I am indebted to my Parents for Living, but to my Teacher for Living Well

—Alexander the Great (356-323 BC)

To my Lovely Bridget

EXECUTIVE SUMMARY

This research involved the development of a human body motion-tracking system constructed with the use of commercial off-the-shelf (COTS) components. This system was initiated to implement a S*ynthetic Environment* (SE) for *Virtual Combat Training* purposes. The main characteristic of a successful SE is the depth of the *immersion* that the users of the SE achieve. The deeper the immersion, the more effective the S*ynthetic Environment* is.

The main component of the system investigated in this thesis was the Control Interface Unit (CIU). The CIU is a component designed to receive data from the magnetic, angular rate, and gravity (MARG) sensors and prepare them to be transmitted through a wireless configuration. A simple and effective algorithm was used to filter the sensor data without singularities, providing the measured attitude in the quaternion form for each human limb. Initial calibration of the MARG sensors was also performed with the use of linear calibrating algorithms. The testing and an evaluation of the whole system was performed by MATLAB® and SIMULINK® simulations and by real-time visualization using a human avatar designed with the X3D graphics specifications.

The MARG sensor used in this research is the third generation of the MARG sensors, called the MARG III sensors. Designed for low power-consumption and size/weight minimization, the MARG III sensors consist of nine micromachined magnetic, angular rate and gravity sensors. The MARG III sensors are programmed to provide measurements with a sampling rate of 100 Hz.

The development of the CIU was completed in stages. First, a one-channel CIU was designed and implemented to handle the data delivered by one MARG III sensor. With this CIU, the MARG system was tested for end-to-end data handling, including data acquisition, data delivery, and wireless data transmission from the MARG III sensor to the 3D projection on a remote screen. Next, the three-channel CIU was developed to test the system's capability of handling

data from multiple MARG III sensors. Finally, the sixteen-channel CIU was designed to facilitate sixteen MARG III sensors. The sixteen-channel CIU is in its final steps of development.

Calibration of the data received by the CIU is performed by linear calibrating algorithms. Precise rotations of the sensors to ensure accurate calibration are performed with the use of a HAAS tilting/rotating table.

The data filtering algorithm chosen is the QUEST algorithm. Already tested in various satellite tracking applications, the QUEST algorithm ensures real-time, efficient data filtering without any singularities. Moderate modifications in the algorithm were made to improve the accuracy of the output with minimal effects in the efficiency of the algorithm.

Through this research, it was discovered that the MARG III sensors had to be redesigned to overcome an erratum on the Honeywell magnetometer HMC1051Z data sheet. With the redesigned MARG III sensors, the testing results showed that the CIU is performing extremely well. The overall motion-tracking system is capable of tracking human body limb motions in real time.

The current system tracks a slow moving human body accurately. All of the experimental results have indicated that after the completion of the sixteen-channel CIU and the complementary filter, the system will be capable of tracking fifteen human limbs accurately. Visual representation and, thus *immersion* into the Virtual Environment, can be achieved without any of the limitations of the previous version of MARG sensors (the MARG II sensors). The 100-Hz sampling rate has proved sufficient for real-time tracking of human body motion. Implementing the system for *immersion* of more than one user into the same Synthetic Environment will also be possible.

I. INTRODUCTION

This chapter discusses the general concept of the MARG project. A brief discussion about the previous work on the project is given, followed by research issues to be addressed in this thesis. Furthermore, a brief outline of the remaining thesis chapters is presented.

A. PREVIOUS WORK ON THE MARG SENSOR

The MARG project is an ongoing effort to achieve the full *representation* of the motion of the human body into a virtual environment, often called a *Synthetic Environment* [Ref. 1]. To be more accurate, the design goal of a *Synthetic Environment* is to make its users feel as if they really exist in that environment. Therefore a more accurate word than *representation* is *immersion*. The deeper the immersion, the more effective the S*ynthetic Environment* is.

The MARG project was designed to implement a S*ynthetic Environment* for *Virtual Combat Training* purposes. Therefore, especially in this case, the depth of the *immersion* is of crucial importance.

An early attempt to create an immersive environment was conducted by Bachman [Ref. 2]. In this dissertation the design of the second generation of a prototype sensor called MARG II (Magnetic, Angular Rate, and Gravity) was described. One MARG II sensor was placed on each human limb to monitor its three-degrees-of-freedom motion. The MARG II sensors consisted of three magnetometers, three accelerometers, and three angular rate micromachined sensors. They were cabled to a central computer, which was used to gather and filter the analog data transmitted from the MARG II sensors and to visually represent the motion of each limb on a human avatar. The system is depicted in Figure 1.

B. RESEARCH ISSUES

The MARG II sensor was not without some drawbacks. First, it was powered by a 12-Volt DC battery, which was enclosed in the casing of the sensor, significantly increasing its size and weight. The power consumption was significant. Therefore, in order to implement a full body motion-tracking system, a sufficient number of battery cells needed to be carried along.

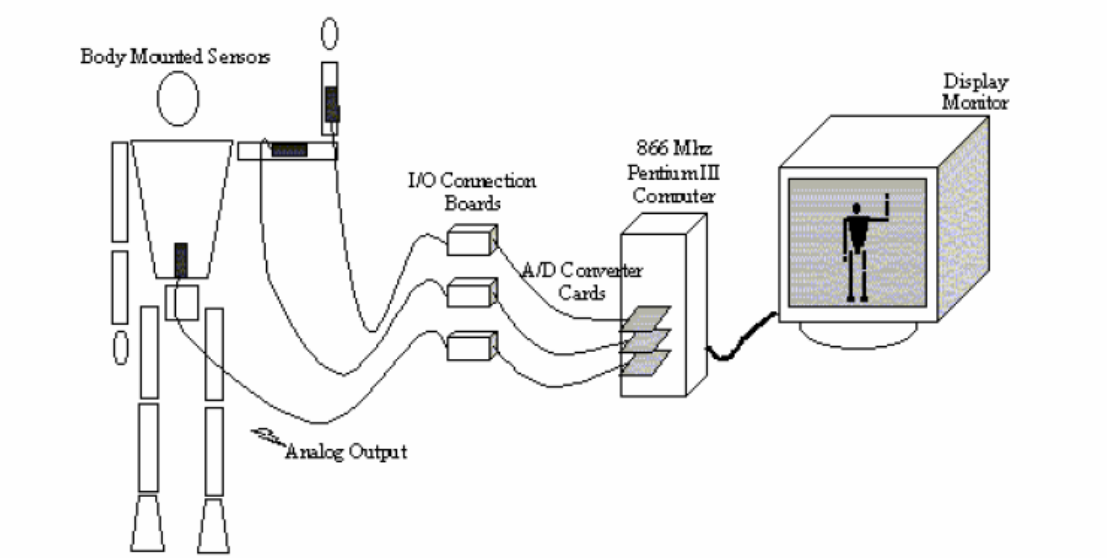

Figure 1. The MARG Project Overview [From Ref. 1.].

Furthermore, the whole structure of the MARG II sensor was based on a single computer that handled all the processes of receiving, sorting, filtering and visually representing the data received from each sensor. A single failure on that computer would totally disrupt the operation of the whole system. If another computer was chosen to replace the original one, a time consuming process of installing drivers and moving bulky hardware from one computer to another would have to occur before the system was again operational. The system performance depended solely on the performance of only one processor.

Another drawback of the MARG II sensor was the permanent attachment of the user to the central computer through the sensor cables, as seen in Figure 1.

Removing the cables from the sensors was cumbersome, since transmitting data wirelessly from all nine data channels for each of the MARG sensors (a total of 135 channels for all 15 MARG sensors) was quite difficult to implement. If the data were in digital format, a multiplexing technique could be used.

The following summarizes the challenges that must be overcome in order to transform the MARG sensor into an easily deployed system:

- Reducing the size and weight,
- Minimizing power consumption,
- Extricating the tracked object from the central computer using wireless transmission,
- Replacing components easily, and finally,
- Decentralizing the computational processes from one central computer to networked multiple components for increased performance and survivability of the system.

In order to resolve the above challenges, the MARG III project was initiated, and the entire system was completely redesigned. The prototype MARG sensors were replaced by a new generation of smaller programmable units, the MARG III sensors. A new component called the Control Interface Unit (CIU) was introduced to remove some of the processing load from the central computer, and also to manipulate the digital data provided by the MARG III sensors and prepare them to be transmitted serially, through a wireless infrastructure. Additionally, the CIU was designed to distribute power to all the sensors from a central battery cell, removing the extra load of a battery from each individual MARG sensor. The sensors and the CIU were designed with low-power consuming components, increasing the durability of the battery cell.

A computer functioning as a server replaced the central computer. This server is capable of establishing a layer 4 (in the OSI model) TCP/IP connection for the initial communication (handshake) between a wireless transmitter, at-

tached to the CIU, and the server. For the actual data flow, a UDP connection is established since real-time data transmission is required. Furthermore, a loss of data packets is not a serious issue in real-time applications in which the data-transmission rate is high enough to overcome those losses.

Finally, for the data representation, another computer was chosen to implement the client, visualizing the body-motion tracking on an avatar designed by using the X3D standard.

C. THESIS GOALS

The main goal of this thesis was to design and to implement the Control Interface Unit (CIU) within the proposed MARG III project and to embed it into the whole MARG III system, which requires the following to be achieved:

- Gather data from the MARG III sensors,
- Feed them to the CIU,
- Transmit them wirelessly to the server,
- Implement a filter to transform the data into rotation angles, and finally,
- Visualize the results on a human avatar.

Due to the extent of the MARG III project effort, this thesis was conducted in parallel with another thesis [Ref. 3], which focuses on a 3-D representation of the motion of the human body.

D. THESIS ORGANIZATION OUTLINE

Chapter II presents the MARG III sensor and its components. A brief discussion reveals the reasons those components were chosen. Particularities concerning the MARG III sensor are addressed.

Chapter III analyzes the Control Interface Unit (CIU). The one- and three-channel CIU and their components are described. The concept of the sixteen-channel CIU is introduced along with the benefits of its implementation.

Chapter IV describes the procedure of uploading the firmware to the MARG III sensor and the CIU. The concept of calibrating the sensors is discussed and the calibrating procedure is described. MATLAB® and SIMULINK® simulations that verify the calibration results are also discussed.

Chapter V conducts the evaluation and testing of the CIU as a functioning part of the whole MARG III project. The QUEST algorithm is used to filter the data delivered by the CIU. Necessary modifications to the algorithm are presented. Finally, combining this thesis work with another thesis [Ref. 3], in an effort to produce a complete MARG III system, is discussed.

The final chapter of this thesis presents conclusions and suggestions for further development and optimization of the results.

E. SUMMARY

In this chapter, the history of the MARG project is discussed along with the drawbacks of the existing MARG sensors and the proposals to overcome those drawbacks. The goals of this thesis were also discussed. Finally a brief summary of the remaining chapters was presented.

THIS PAGE INTENTIONALLY LEFT BLANK

II. THE MARG III SENSOR

This chapter provides a brief discussion of the MARG III sensor and its components. The MARG III sensor consists of three accelerometers, three magnetometers, three rate sensors, and a Texas Instruments (TI) microcontroller.

The three accelerometers form an orthogonal triad and so do the three magnetometers and rate sensors. The three different triads are placed on the sensor's Printed Circuit Board (PCB) forming three right-handed coordinate systems. All of the sensor triads are aligned with each other. Therefore, the orientation of the accelerometer pointing in the positive *x*-axis coincides with those of the magnetometer and the rate sensor pointing in the positive *x*-axis. The sensors pointing in the positive *y*- and *z*-axis follow the same convention, yielding a right-handed coordinate system *body frame* for the designed MARG III sensor.

A. PERFORMANCE REQUIREMENTS

In order to justify the reason for choosing each of the components, a brief analysis of the human body motion is presented below.

The fact that the human arm is the fastest moving human limb is commonly known. Therefore if the limits satisfy the arm's performance requirements, then all other limb limitations will also be satisfied. Normally, the maximum tangential speed that a human wrist can accomplish is no greater than 3 m/sec and its maximum acceleration fluctuates between 5 and 6 g [Ref. 2]. A grenade throwing motion, which is a classic case of a really fast arm motion, is usually achieved with tangential velocities greater than 35 m/sec and accelerations of more than 25 g [Ref. 2]. The bandwidth occupied by the normal arm motion is estimated to be close to 2 Hz, whereas faster motions may spread the bandwidth to approximately 5 to 6 Hz. When the human arm moves as a result of a neuromuscular reflex motion, then a 10-Hz approximation of the bandwidth is consid-

ered to be accurate [Ref. 2, 4]. Therefore, the sampling rate required to avoid aliasing according to the Nyquist theorem should be 20 Hz.

Furthermore, the components of the project, especially the sensors, are expected to be susceptible to noise. Therefore, the computed sampling rate is multiplied by a *safety* factor. Following a general rule of thumb of oversampling 20 times, aliasing will be avoided [Ref. 2]. This results in a sampling rate of 200 Hz for the 10 Hz bandwidth of the reflex motions. The normal human motion of 5 Hz bandwidth results in a sampling rate of 100 Hz, which is implemented in the MARG III sensor. With the above in mind, the following components were chosen for the MARG III sensor.

B. THE HONEYWELL HMC1051Z/HMC1052 ONE- AND TWO-AXIS MAGNETIC SENSORS

The following material is mainly taken from [Ref. 5].

Honeywell has created a family of one-, two-, and three-axis magnetic sensors. At the time the MARG III was designed, the three-axis magnetic sensor was not yet available. Therefore in the MARG III design, a pair of the two-axis (HMC1052) and one-axis (HMC1051Z) magnetic sensors was chosen for *x*- and *y*-axes and *z*-axis, respectively, to create the magnetic sensor triad. The dimensions of the one-axis HMC1051Z are 6.850 x 9.829 x 1.371 mm, whereas those of the two-axis HMC1052 are 4.75 x 2.90 x 1.10 mm. A magnified view of the two sensors is shown in Figure 2.

Although the two-axis magnetic sensor is smaller in dimension than the one-axis one, a pair of a HMC1052 and a HMC1051Z proved most suitable because Honeywell has designed them to create an orthogonal triad when mounted on the same PCB [Ref. 5].

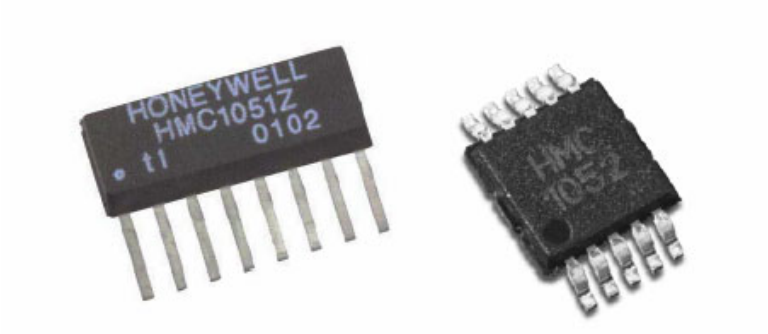

Figure 2. The Honeywell Magnetic Sensors HMC1051Z and HMC1052 [From Ref. 5.].

The sensors are designed as 4-element Wheatstone bridges, which are capable of converting very low magnetic fields to differential voltages. In fact they can detect magnetic fields of only 120 μgauss in strength.

Besides the bridge circuit, the HMC1051Z and HMC1052 micromachined magnetoresistive sensors have two onboard magnetically-coupled straps, the off-set strap and the set-reset strap.

The purpose of the offset strap, attached to the entire circuit, is to provide different modes of operation such as:

- Eliminating the unwanted magnetic fields residing in the area where the sensor operates,
- Nulling the bridge offset voltage,
- Canceling the closed-loop field, and finally,
- Auto calibrating the bridge gain.

In most applications (including MARG III) the offset strap is not used. Therefore the offset strap connections have been left open-circuited, as suggested by Honeywell [Ref. 5].

The set-reset strap, when driven properly, provides the sensor with a polarity flip of the Wheatstone bridge output voltage (and therefore north-south flip).

A “set pulse” is defined as a positive pulse current of approximately 400 mA over the nominal resistance of 3 to 6 ohms that the strap provides, when applied on the set-reset positive strap connection. On the other hand, a “reset pulse” is defined as a negative pulse current of approximately 400 mA, applied also on the set-reset positive strap connection. When applying a reset pulse, the magnetic domains produce negative voltages across the output connections. A set pulse does exactly the opposite, and when applied following the order reset-set within a few milliseconds, the magnetic domains reverse their direction twice, thereby canceling any prior remaining magnetic fields that may reside on them.

1. Particularities for the MARG III Design

Unfortunately, Honeywell designed the one- and two-axis magnetic sensors to form a triad that follows the left-handed coordinate system. The two coordinate systems (left- and right-handed) differ in the orientation of *z*-axis. Therefore, in order to transform the coordinate system of the magnetic sensors from a left-handed to a right-handed system, the orientation of the HMC1051Z, which plays the role of the *z*-axis magnetometer, must be flipped.

One way to do this is by programming this sensor to set-reset periodically instead of reset-set. That would result in a 180^{o} *z*-axis flip. Another method is to place the HMC1051Z upside down (belly up) on the PCB, so as to point to negative *z* instead of positive *z*. By doing that, the set-reset straps in both HMC1052 and HMC1051Z magnetometers are used in a coherent way (both of them in a set-reset sequence). The latter is the solution chosen for the MARG III sensor.

C. THE ANALOG DEVICES ADXL202E TWO-AXIS ACCELERATION SENSOR

The following material is mainly taken from [Ref. 6].

The accelerometers chosen for the MARG III design were the micromachined two-axis acceleration sensors ADXL202E from Analog Devices shown in Figure 3 [Ref. 6]. They have a measurement range of static and dynamic ac-

celerations of 4 g (±2 g), which was considered sufficient for measuring typical human motions.

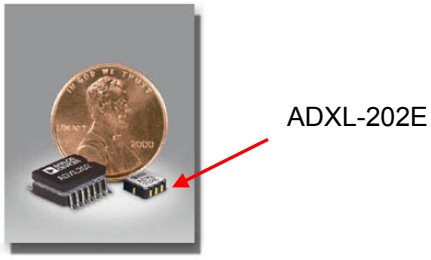

Figure 3. The ADXL202E Two-axis Acceleration Sensor [After Ref. 7.].

Their size is 4.50 x 5.00 x 1.78 mm. Since each chip can sense acceleration in two orthogonal dimensions, only two of them are required in order to form an orthogonal triad.

The block diagram of ADXL202E is shown in Figure 4, which illustrates that this sensor is capable of providing both analog (from C_x and C_y capacitors) and digital output (from X_{out} and Y_{out}). When the C_x and C_y capacitors are not used to drive the analog output, they can be used to determine the bandwidth of the accelerometer. More information on the bandwidth will be presented later.

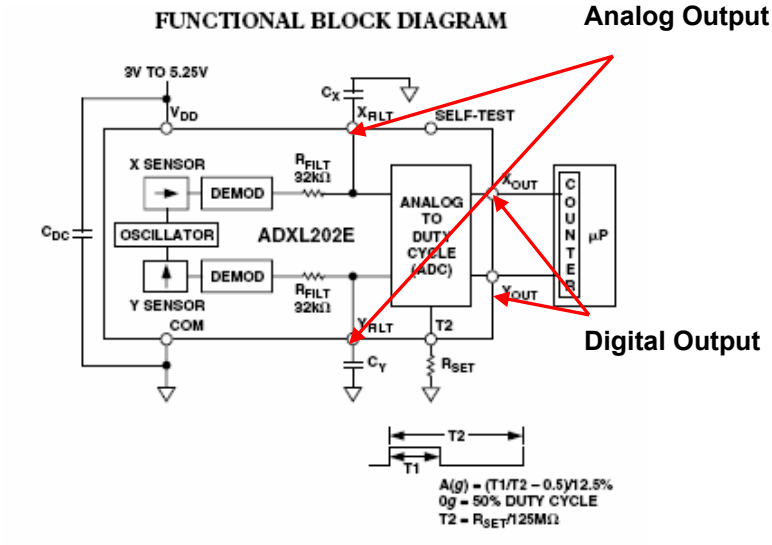

Figure 4. Functional Block Diagram of ADXL202E Acceleration Sensor [After Ref. 6.].

The digital output is represented by the duty cycle of the pulses created by the oscillator, which is directly proportional to the combination of the dynamic and static acceleration measured by the sensors.

The duty cycle is the ratio of the pulsewidth T_1 over the period of the pulse T_2, and can be directly fed to a microcontroller along with T_2, to recompute the measured acceleration.

1. Defining the Bandwidth and the DCM (Duty-Cycle Modulation) Period of the Sensor

By choosing the correct values for capacitors C_x and C_y, the bandwidth of the measurement can be defined. By doing that, low-pass filtering is achieved in order to improve the measurement resolution and to help prevent aliasing [Ref. 6].

Table 1 lists the value of bandwidth for several values of C_x and C_y. The minimum allowed value for C_x and C_y is 0.001 µF. For the MARG III sensor, the C_x and C_y were chosen to be 0.027 µF, providing a bandwidth for the sensor output of 200 Hz.

Bandwidth	Capacitor Value
10 Hz	0.47 µF
50 Hz	0.10 µF
100 Hz	0.05 µF
200 Hz	0.027 µF
500 Hz	0.01 µF
5 kHz	0.001 µF

Table 1. Filter Capacitor Selection C_x and C_y [From Ref. 6.].

2. Particularities for the MARG III Design

Figure 5 shows that, when an axis (e.g., *x*) is pointing down (negative 90°), the sensor is configured to provide positive values of acceleration.

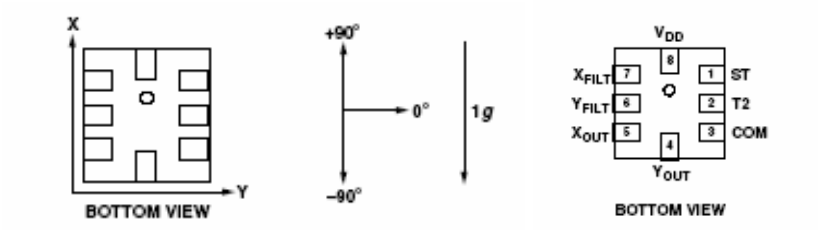

Figure 5. Polarity Convention and Coordinate System Definition on ADXL202E Acceleration Sensor [From Ref. 6.].

As mentioned previously in this chapter, the MARG III design follows the right-handed coordinate system. Unfortunately, the triad formed by the pair of the two ADXL202E follows the left-handed coordinate system. In order to overcome this problem, the accelerometers were placed upside down on the MARG III PCB yielding a right-handed coordinate system.

This orientation endowed the MARG III with a particularity. When an axis (e.g., *x*) is pointing down (tilted 90^{o} from the horizontal plane toward the ground), the output of the corresponding gravity sensor is a positive 1 g. Similarly, when pointing up, the output is a negative 1 g.

D. THE TOKIN CG-L43 CERAMIC GYRO

The following material is mainly taken from [Ref. 8].

The rate sensor chosen for the MARG III design was the CG-L43 ceramic gyro designed by NEC/TOKIN. It is a miniature, high-speed response, magnetic field-proof sensor. This gyro consists of a single piezoelectric ceramic column printed with electrodes, which when supplied with +3 V, can detect a maximum angular rate of $\pm$90 deg/sec, at a nominal ambient temperature of 25^{o} C [Ref. 8].

With dimensions of 8 x 16 x 5 mm, the CG-L43 was the smallest rate sensor available on the market at the time the MARG III was designed. Today, NEC/TOKIN offers the next generation of ceramic gyros CG-L53, with dimensions 6 x 10 x 2.5 mm. Keeping in mind that these gyros are in fact the bulkiest component of the MARG III, substituting the CG-L43 for another sensor, probably

a CG-L53, will benefit the next versions of the MARG sensor by reducing its size and weight. The CG-L43 and CG-L53 are shown in Figure 6.

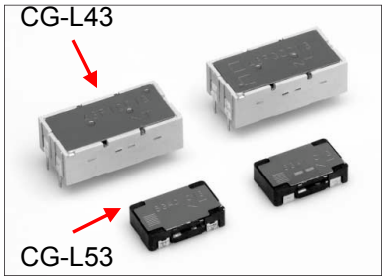

Figure 6. The CG-L43 and CG-L53 Ceramic Gyros [After Ref. 8.].

Since the rate sensors are not used at this phase of the MARG III project, they will not be discussed further. In this thesis the measurements from the magnetic sensors and the accelerometers are acquired, processed, and analyzed.

E. THE TEXAS INSTRUMENTS MSP430F149 MICROCONTROLLER

Two of the three components of the MARG III (the magnetometers and the rate sensors) produce analog data. Therefore, the MARG III needed another component to implement the analog-to-digital conversion and to transmit the digital data to the CIU.

After an extensive trade-off analysis, the Texas Instruments MSP430F149 microcontroller was selected and incorporated into the sensor unit [Ref. 9]. It is an Ultra Low-Power 16-bit RISC architecture with a 125-ns Instruction-Cycle Time and a hardware multiplier. It operates with a very low supply voltage that can vary from 1.8 Volts to 3.6 Volts. It has three modes of operation [Ref. 10]:

- An Active Mode: 280 μA at 1 MHz, 2.2 Volts,
- A Standby Mode: 1.6 μA, and
- An Off Mode with RAM detention: 0.1 μA.

When designing the MARG III sensor, one of the tasks was how to connect the three magnetometers, the three rate sensors and the three accelerometers into one microcontroller. Among the 48 I/O pins of the MSP430F149 microcontroller, eight pins are reserved for analog inputs and are designed to drive the input of a 12-bit A/D converter [Ref. 11]. Therefore the six analog signals provided by the magnetometers and the rate sensors could be connected to six of those eight I/O pins.

Furthermore, the digital output from the accelerometers could be interfaced to the three capture-compare registers of one of the two timer-modules (Timers A3 and B7; the latter is being used in the MARG III design). Owing to this combination, the need to use a more complicated microcontroller with at least 12 or 16 analog channels was avoided.

Another attractive feature of the MSP430F159 is the relatively large RAM of 2 KB and the quite large memory of 60 KB+256 B (program and data, respectively) [Ref. 10]. This gives the MARG III user the capability of writing code for the microcontroller, testing it, improving it, and uploading it into the microcontroller's flash memory without any additional hardware changes. In an extreme case, if something is found to be wrong in the hardware design of the MARG III, the microcontroller itself will not need to be modified; only new firmware that corresponds to the changes will need to be uploaded.

Finally, the MSP430F149 offers two universal serial synchronous-asynchronous communication interfaces (USART) that enable the microcontroller to communicate with its subsequent units. These are the MSP430F149 inside the CIU (communication between the MARG III and the one-channel CIU) and an RS-232 module (communication between the one-channel CIU and the Wiser 2400 wireless transmitter). The microcontroller onboard the MARG III communicates with the one-channel CIU by using the SPI Synchronous mode.

F. THE MARG III MAGNETIC, ANGULAR RATE AND GRAVITY SENSOR AS AN ENTITY

After the MARG III sensor design was finalized, McKinney Technology was contracted to fabricate the sensors.

The top and bottom views of the MARG III prototype boards are shown in Figure 7, which shows how small the MARG III PCBs are compared to an American quarter.

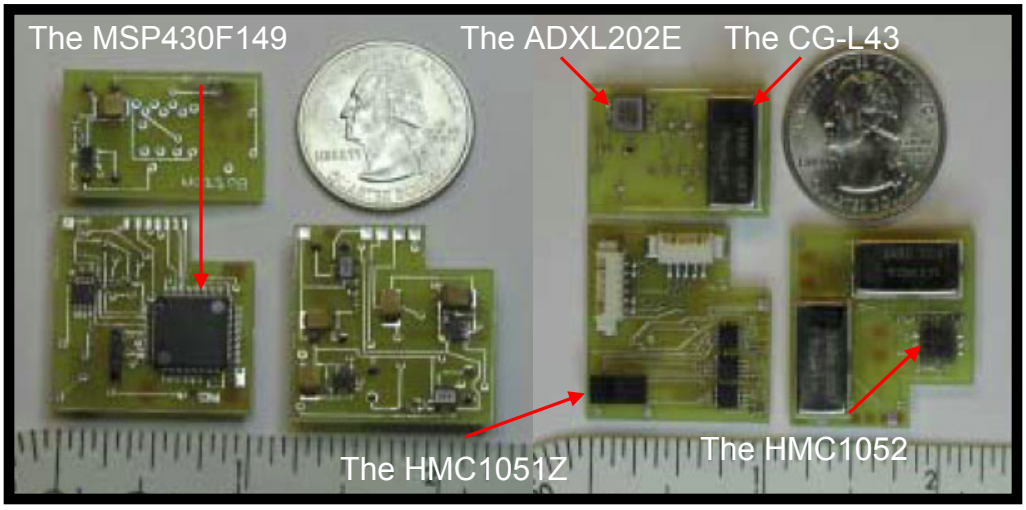

Figure 7. Top (left) and Bottom (right) View of the Manufactured MARG III Prototype [After Ref. 9.].

Figure 8 shows the top, bottom, and side views of the MARG III assembled into a one-piece sensor unit.

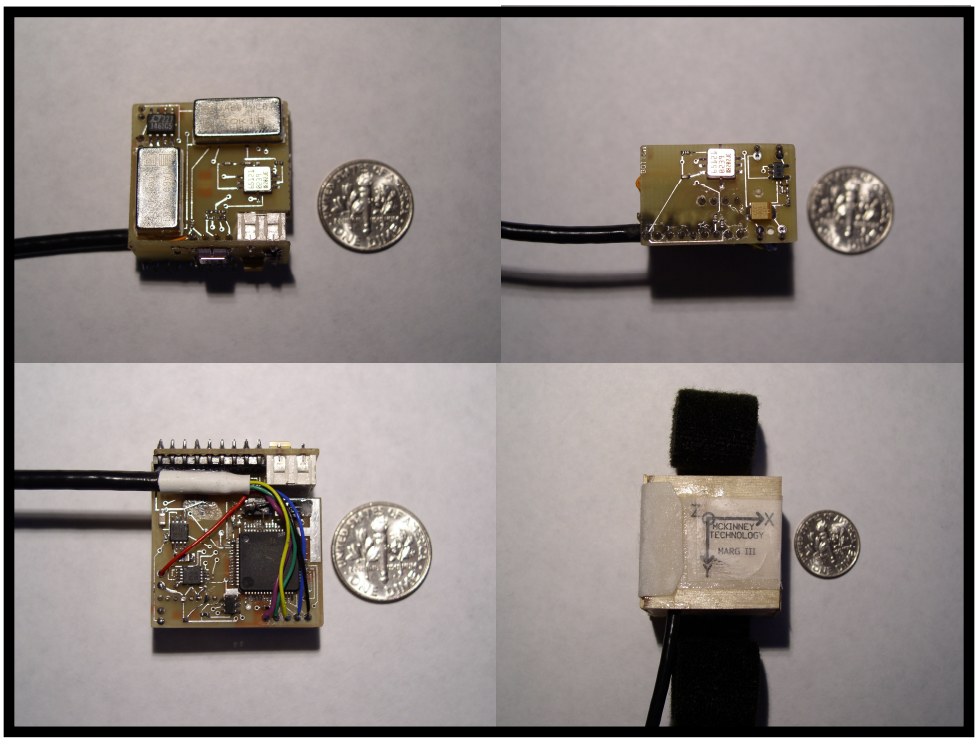

Figure 8. The Manufactured MARG III Unit (Compared to a Dime).

The dimensions of the MARG III are 28 x 30.5 x 17.3 mm. When placed inside the box shown in Figure 8, its size becomes 31.75 x 30.2 x 23.8. Without the box, it weighs approximately 8.5 grams (0.3 oz). It consumes 144 mW (20 mA) when powered with 7.2 Volts. It can operate within a range between 5.5 and 8 Volts. It provides nine digital outputs using 12-bit words with a sample rate of 100 Hz.

G. SUMMARY

This chapter discussed the MARG III components, their physical arrangement aboard the sensor's PCB, and their main characteristics. The performance requirements for the micromachined sensors and the microcontroller were analyzed, and the final form of the MARG III sensor was presented.

In the following chapter the one- and three-channel Control Interface Unit (one- and three-channel CIU) will be analyzed. The concept of the sixteen-

channel CIU will be presented along with the benefits of its implementation in the system.

III. THE CONTROL INTERFACE UNIT (CIU)

Chapter II described the hardware design of the MARG III sensor. This chapter discusses the Control Interface Unit (CIU). First, the purpose of using the CIU is presented. Then a description of the one- and three-channel CIU is given. Finally, the approach for designing and implementing a sixteen-channel CIU is presented.

A. PURPOSE OF THE CONTROL INTERFACE UNIT

The Control Interface Unit (CIU) was designed to remove part of the computational load from the MARG II central computer, as mentioned in Chapter I. The main purpose, though, was to prepare the MARG III data to be transmitted wirelessly. In order for this to be achieved, multiplexing of the data from all nine channels of each sensor was necessary.

The MARG II sensor was powered by an onboard battery cell. The MARG III sensor has been designed with the goal of minimizing size and weight. Therefore, the need for an external power supply emerged.

The data from the MARG III sensor must be multiplexed in order to be sent serially through a single transmission channel. Furthermore, in order to achieve the detachment of the MARG III sensors and the CIU from the rest of the hardware components of the MARG III project, the serial data must be transmitted wirelessly. Therefore, the CIU has to deliver the data in a format that is easy to transmit wirelessly.

The MARG III sensor communicates with the CIU through a Universal Synchronous Asynchronous Receiver Transmitter (USART) operating in the Synchronous Peripheral Interface (SPI) mode. In this configuration the MARG III sensor operates as a *slave device* whereas the CIU is the *master device*. This means that the clock signal needed for synchronizing the data transmission has to be delivered to the MARG III sensor by the CIU.

B. THE ONE-CHANNEL CONTROL INTERFACE UNIT (ONE-CHANNEL CIU)

It was very difficult for all aforementioned functions to be achieved with a single stage. Therefore, the CIU had to be designed and implemented in stages. First, the MARG III data acquisition had to be achieved from a single MARG III sensor. Then the data had to be forwarded through the wireless channel and received by a server program capable of filtering the data. The visual representation of the data delivered by one MARG III sensor had to follow. Finally, the remaining goal was receiving and multiplexing the data from all sixteen MARG III sensors.

For these reasons, the one-channel CIU was designed and implemented first. A picture of the one-channel CIU is shown in Figure 9. The main component of the one-channel CIU is a TI MSP430F149 microcontroller identical to the one onboard the MARG III sensor. This microcontroller was chosen for the same reasons it was included in the MARG III sensor design: low power consumption, UART-USART capabilities, small size and weight, programmability, etc.

The one-channel CIU can operate with any power supply within the range of 7 to 9 Volts. For field applications a 9-Volt battery cell can be used. Alternatively, for testing purposes, a power supply unit operating within the range of 7 to 9 Volts can be used.

The CIU connects to the MARG III sensor through the connector shown with a blue arrow in Figure 9. As mentioned above, communication is established by using the SPI mode of the USART interface of the TI microcontroller. A 5.120 MHz crystal, shown in Figure 9 with a red arrow, is used to provide the clock needed to synchronize the SPI communication.

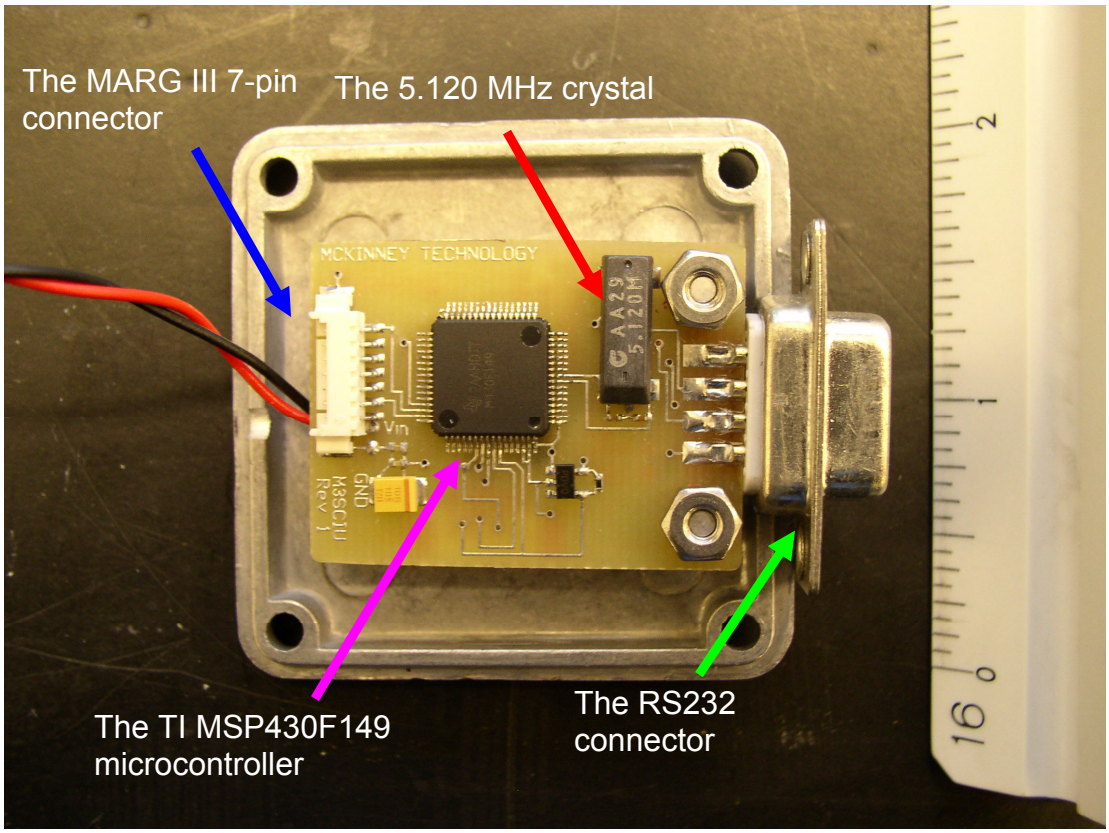

Figure 9. The One-channel Control Interface Unit (One-channel CIU).

The device selected to transmit the data wirelessly from the CIU to the computer running the server program is a Wiser 2400 serial-to-wireless transmitter [Ref. 12]. The input to this device must be in RS232 format. Therefore, the one-channel CIU was equipped with a MAX3238 TTL-to-RS232 converter [Ref. 13], capable of converting the UART output from the TI microcontroller to standard RS232 format at a transmission rate of 19.2 kbps.

The MAX3238 converter is shown with a red arrow in Figure 10. The output from the MAX3238 converter is in the form of 10-bit words (8-bit payload, one start-bit, one stop-bit, and no parity bit), with no flow control.

Figure 11 shows the schematic diagram of the cable connection between the MARG III sensors and the CIU. The CIU receives the data from the MARG III sensor through an SPI communication interface. Then, the data are fed to the

MAX3238 converter through the TI MSP430F149 microcontroller's USART interface. From that point, the Wiser 2400 is responsible for the wireless transmission of the data.

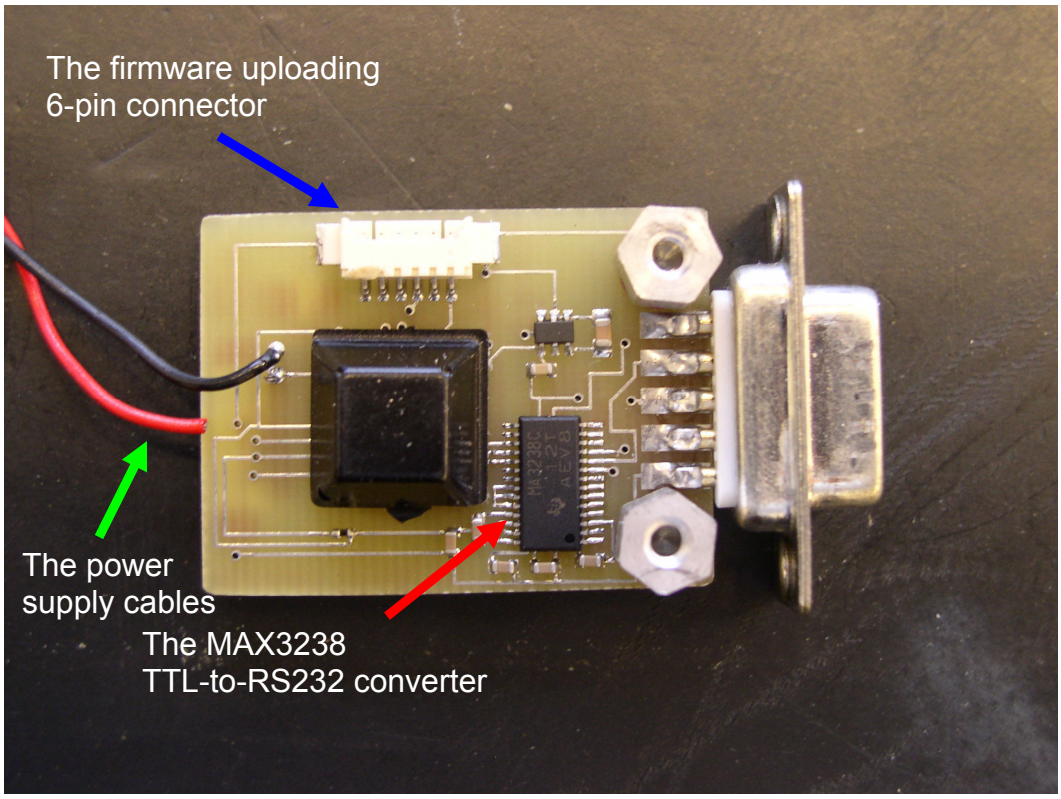

Figure 10. Bottom View of the One-channel Control Interface Unit (One-channel CIU).

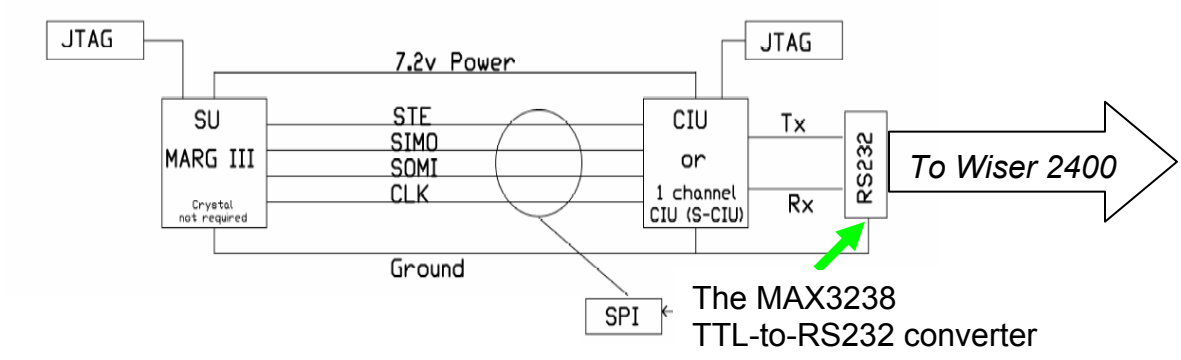

Figure 11. The MARG III – CIU Schematic [After Ref. 14.].

C. THE THREE-CHANNEL CONTROL INTERFACE UNIT (THREE-CHANNEL CIU)

After the one-channel CIU was designed, developed and implemented, there was a need to test the system with multiple MARG III sensors. The purpose of building the three-channel CIU was to test the visual representation of multiple limb tracking and also the *wireless transmission* configuration. For these tests to be performed, the three-channel CIU was designed.

The three-channel CIU is shown in Figure 12. The three-channel CIU is constructed from three one-channel CIUs in a parallel configuration.

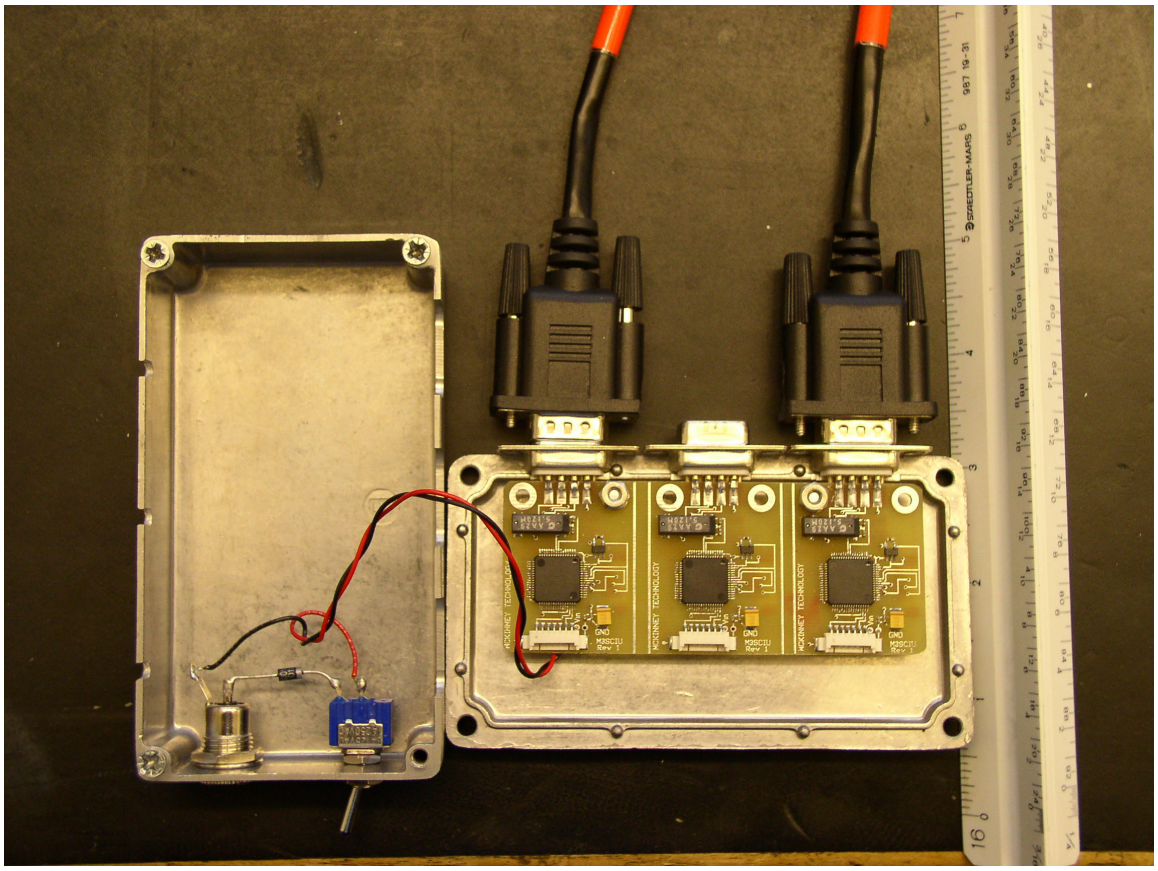

Figure 12. The Three-channel Control Interface Unit (Three-channel CIU).

D. THE SIXTEEN-CHANNEL CONTROL INTERFACE UNIT (SIXTEEN-CHANNEL CIU)

In an effort to transmit the data delivered by all the MARG III sensors, the sixteen-channel CIU was designed. Even though the MARG III project is designed to track fifteen limbs of the human body, a sixteenth connection was designed in case there was a need to track an additional motion without fundamental hardware changes.

In addition to the purposes served by the one- and three-channel CIU, the main purpose of the sixteen-channel CIU was to route the data delivered from the MARG III sensors through a single wireless communication channel. For this reason, various methods of multiplexing were studied. The selected method was to use a XILINX® Spartan™-II XC2S100 Field Programmable Gate Array (FPGA) [Ref. 15]. The prototype board of the sixteen-channel CIU is shown in Figure 13 and in Figure 14.

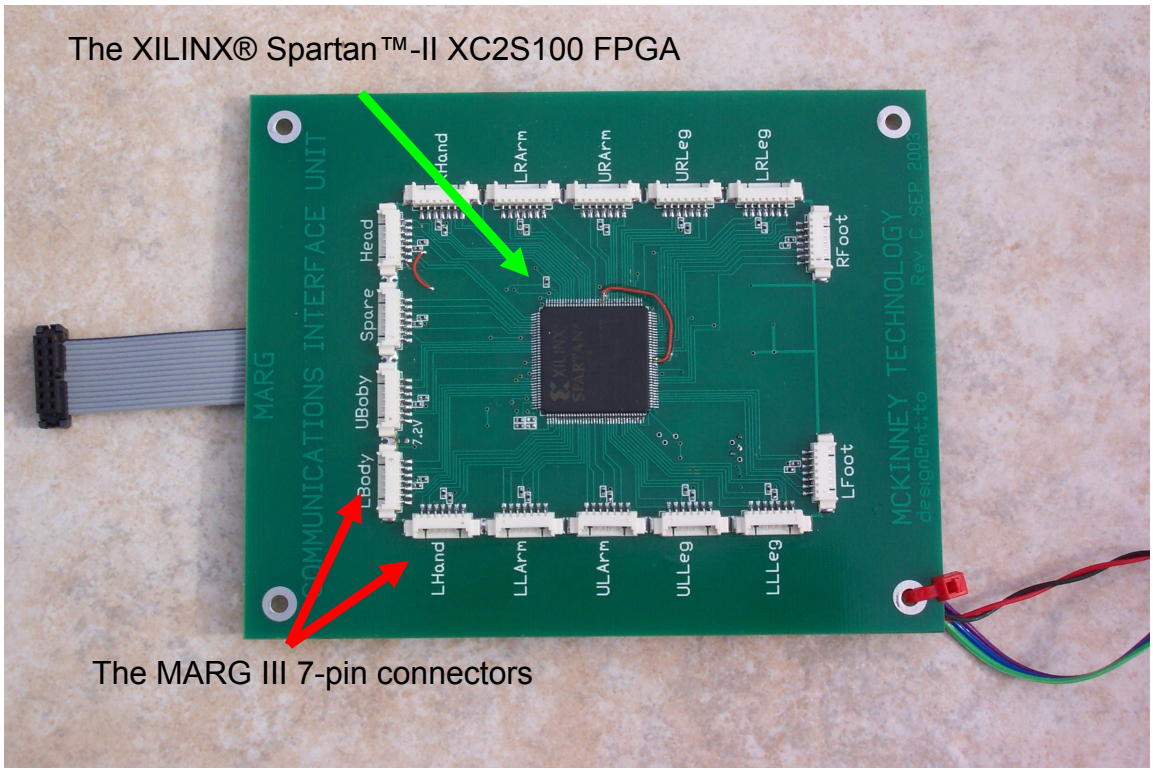

Figure 13. Top View of the Sixteen-channel Control Interface Unit (Sixteen-channel CIU).

Figure 13 shows the top view of the sixteen-channel CIU with the XC2S100 FPGA, along with the sixteen MARG III sensor connector pins. Figure 14 shows the bottom view of the sixteen-channel CIU. The TI MSP430F149 microcontroller is shown with the green arrow. The red arrow shows the connector cable for programming the FPGA, and the blue arrow shows the connector for uploading the firmware to the microcontroller. Finally, the black arrow shows the serial-output cables.

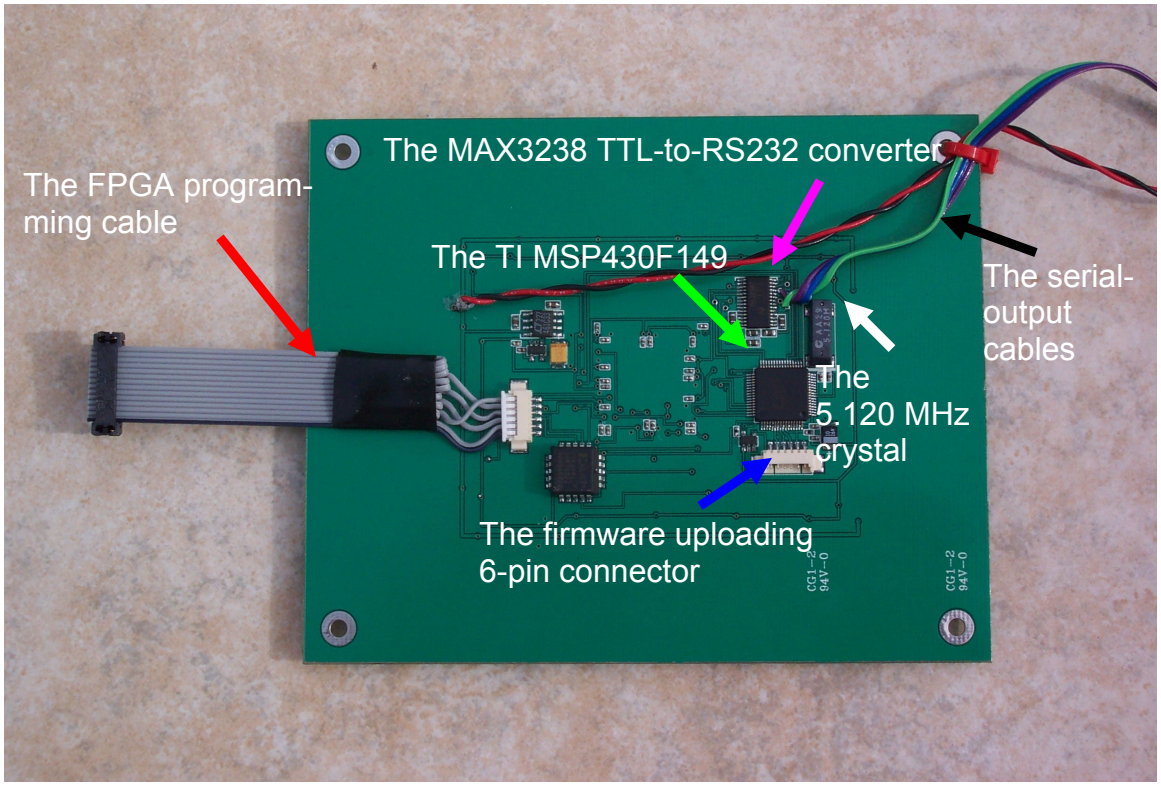

Figure 14. Bottom View of the Sixteen-channel Control Interface Unit (Sixteen-channel CIU).

The MARG III data are fed directly to the XC2S100 FPGA. None of the MARG III sensors transmits data unless the FPGA commands them. The connection between the MARG III sensors and the FPGA is achieved through SPI communication, following the configuration shown in Figure 11. The TI microcon-

troller is responsible for providing the clock needed. The 5.120 MHz crystal, shown in Figure 14 with a white arrow, provides the necessary clock signal to the TI microcontroller.

After the data are received from the MARG III sensors, they are multiplexed by the FPGA and packaged into 232-byte words, as shown in Table 2, including the payload from all sixteen MARG III sensors and the necessary overhead to establish robust communication. In the event that one or more MARG III sensors are not connected or that they transmit incorrect data, the FPGA replaces the respective bits with zeros in order to keep a constant transmission rate of 232 kbps.

The payload for each one of the sixteen MARG III sensors consists of the information transmitted from the three magnetic (M_x, M_y, M_z), the three angular rate (R_x, R_y, R_z), and the three acceleration sensors (A_x, A_y, A_z) onboard the MARG III sensor (nine channels for each sensor). Each channel (transmitted in the order of R_x, R_y, R_z, A_x, A_y, A_z, M_x, M_y, M_z) occupies one and a half byte, giving a total of 13.5 bytes of payload for each MARG III sensor. To this payload an identification number of a half a byte must be added to associate the data received with the corresponding MARG III sensor. This ID number leads to a total payload of 14 bytes for each MARG III sensor.

Number of Bytes	***Content***
2	Communication Synchronization
2	MARG III "Alive" Identification Bits
2	Payload "Health" Status
1	Timing
1	Sample Number
(13.5 + 0.5) x 16 MARG III sensors (Total of 224 bytes)	Payload and MARG III Identification Number
Total: 232 Bytes	

Table 2. The Sixteen-channel CIU Output Byte-format.

Unfortunately, the commercially designed RS232 products do not support data rates higher than 115 kbps. Therefore, a custom made RS232 serial to wireless transmitter is under development. For maximum flexibility, though, the sixteen-channel CIU has been designed in such a way that the MAX3238 TTL-to-RS232 converter (shown in Figure 14 with a purple arrow) can be easily bypassed with minimal hardware changes. This small change enables the CIU to provide output through a UART configuration, which theoretically can support the 232-kbps transmission rate.

E. SUMMARY

This chapter discussed the purpose of designing a Control Interface Unit (CIU). The one- and three-channel CIU was presented and the sixteen-channel CIU was introduced. The following chapter discusses the process of uploading firmware to the MARG III sensors and the one- and three-channel CIU. The process of conducting initial calibration to the components of the MARG III sensors will be discussed as well.

THIS PAGE INTENTIONALLY LEFT BLANK

IV. FIRMWARE UPLOADING AND CALIBRATION

The hardware components of the MARG III sensors were described in Chapter II, and the one- and three-channel CIUs were presented in Chapter III, along with the sixteen-channel CIU. This chapter presents the process of loading firmware to the MARG III sensors and the CIU. It also addresses the process of conducting the initial calibration.

A. UPLOADING THE FIRMWARE

The MARG III sensors and the CIUs are not Application Specific Integrated Circuits (ASICs) [Ref. 16]. Therefore, in order to perform the specific actions they were designed for, firmware must be uploaded to the TI MSP430-F149 microcontrollers. The MARG III firmware enables the microcontroller to do the following:

- Acquire (sample) the data from each analog micromachined sensor,
- Convert the duty-cycle output of the accelerometers into digital voltage corresponding to gravity measurements,
- Parse the measurements into 12-bit words, and finally,
- Transmit those words through a Serial Peripheral Interface (SPI-slave) to the CIU.

The CIU firmware achieves the following:

- Provides the clock for the MARG III sensor,
- Commands the MARG III sensor to send data (SPI-master),
- Receives the data, and finally,
- Forwards the data to the MAX3238 TTL-to-RS232 converter onboard the CIU.

The MARG III sensors and the one- and three-channel CIU were delivered without the required firmware. A separate subcontractor was hired by McKinney Technology to create the firmware needed.

In order to program the microcontrollers, the Texas Instruments MSP-FET430P140 tool was used. The tool includes the hardware and the software to erase and to program the MSP430F149 flash memory. It has an integrated software environment and connects directly to the parallel port of a PC. This procedure greatly simplifies the setup and the use of the tool and therefore the programming of the MSP430F149 onboard the MARGIII sensors and the CIUs.

The MSP-FET430P140 includes:

- 2 MSP430F149 flash devices,
- A FET-to-PC adapter,
- Header pinouts for prototyping,
- Integrated IAR Kickstart user interface, which includes an assembler, linker, simulator, source-level debugger, and limited C compiler, and
- A LED indicator and MSP430F13x/14x FET development board with ZIF socket.

The MSP-FET430P140 development tool is shown in Figure 15. The development board was used to become acquainted with the procedure of programming the flash memory. In order to program the microcontrollers onboard the sensors and the CIU directly, a custom-made JTAG cable was constructed. This cable connected the FET with the sensors and the CIU directly. Additionally, the more functional IAR full-version Workbench (user interface) was purchased to replace the Kickstart version.

Figure 16 shows the configuration used to program the microcontrollers directly. The red arrow in the same figure points to the custom made JTAG cable that connects the MARG sensor to the CIU firmware connectors.

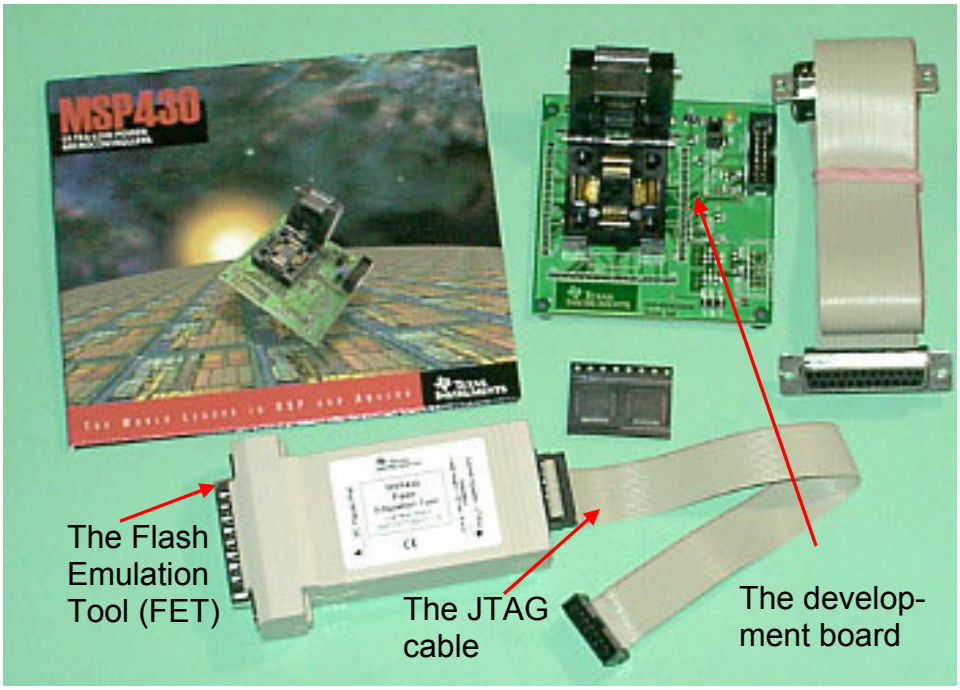

Figure 15. The Texas Instruments MSP-FET430P140 Development Tool [From Ref. 17.].

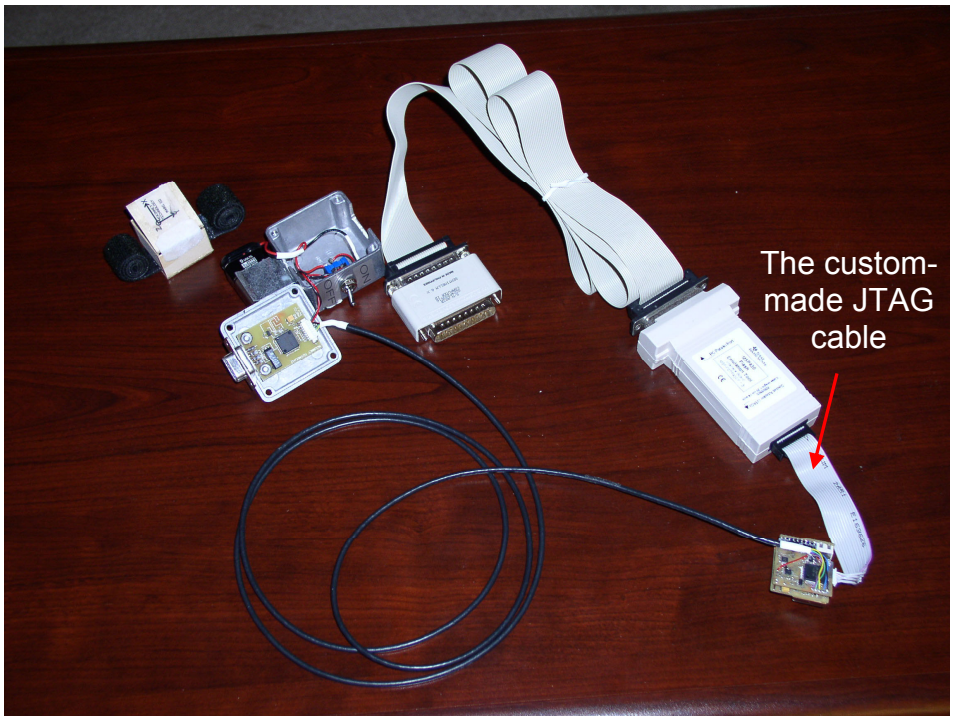

Figure 16. The Configuration Used to Program the Microcontrollers.

1. Preparing the Workbench – Firmware Upload

Both the MARG III sensor and the CIU firmware were delivered in the format of an *IAR Embedded Workbench Project*. In order to upload the firmware to the microcontrollers, the User Interface needed to be initialized. The goal of the initialization process was to *inform* the interface that the *target* was a TI MSP430F149 microcontroller. Furthermore, the directories where the *libraries* and all other needed files are located are specified.

The Interface comes with its own default values for all the parameters. The ones that must be changed are described below.

Figure 17 shows where the options menu can be found. When activated, the menu looks as shown in Figure 18. The *device with hardware multiplier* should be chosen in the *processor configuration* drop-down menu.

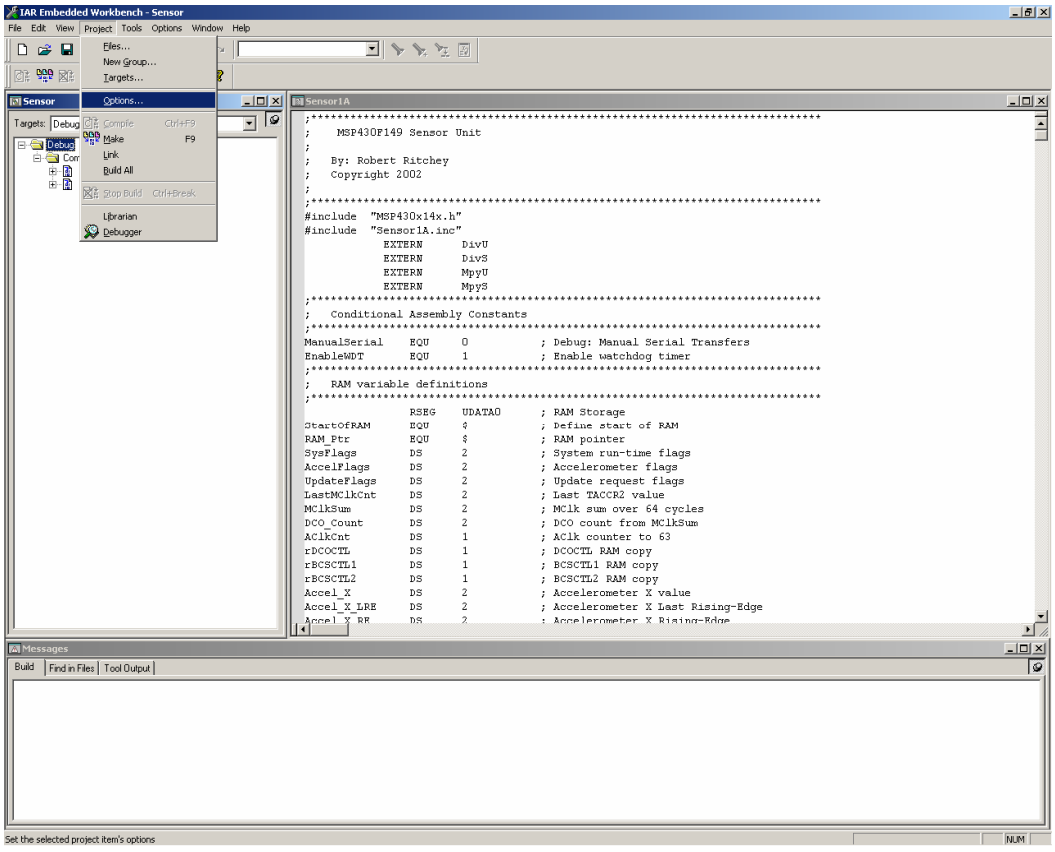

Figure 17. Options Menu on the IAR Embedded Workbench.

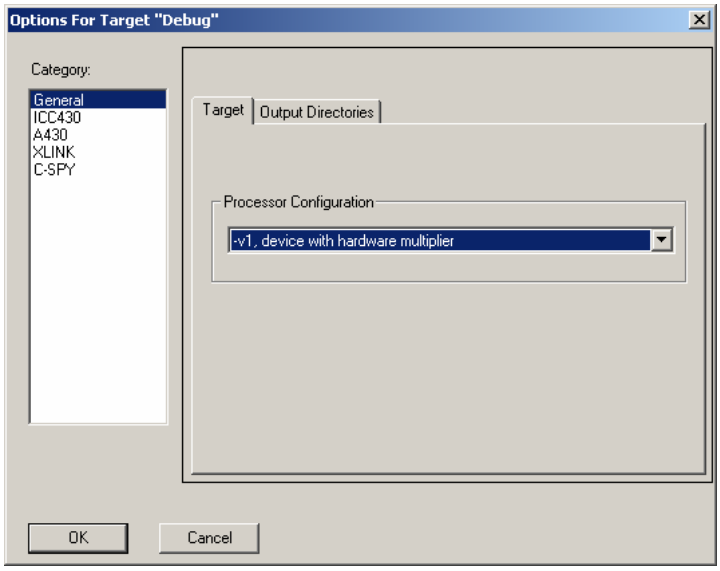

Figure 18. General Submenu in the Options Menu.

Next, in the ICC430 submenu two tabs should be updated, the *Code Generation* and the *Include* tab. When updated, they should look as shown in Figure 19.

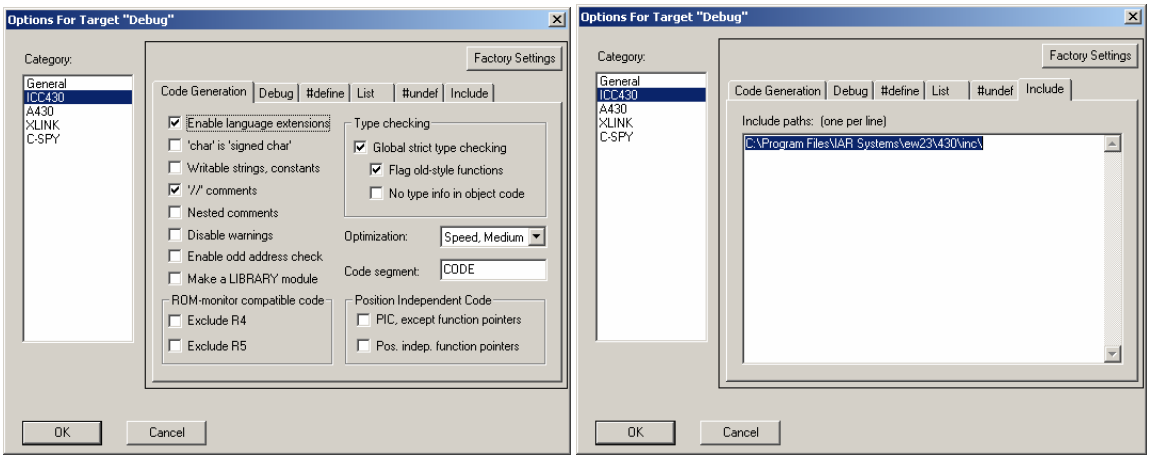

Figure 19. ICC430 Submenu in the Options Menu.

In the A430 submenu, the *Include* tab should be updated as shown in Figure 20. Finally, Figure 21 and Figure 22 show the necessary changes that must be done in the XLINK and C-SPY submenus.

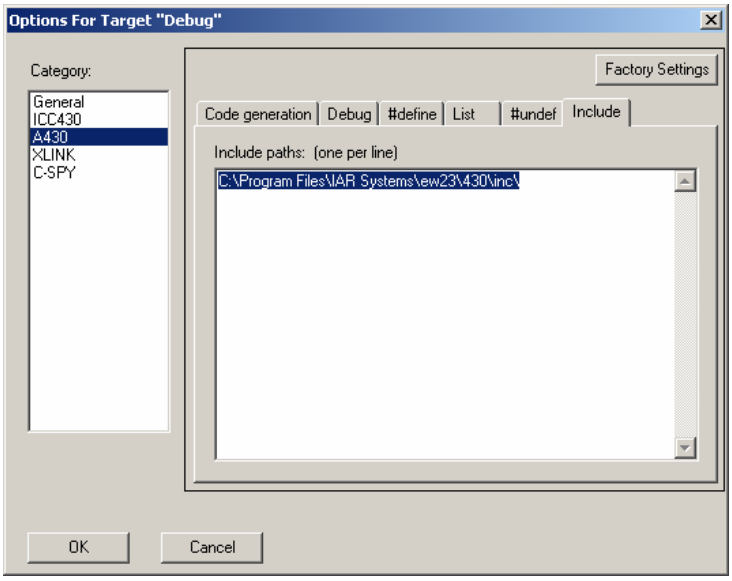

Figure 20. A430 Submenu in the Options Menu.

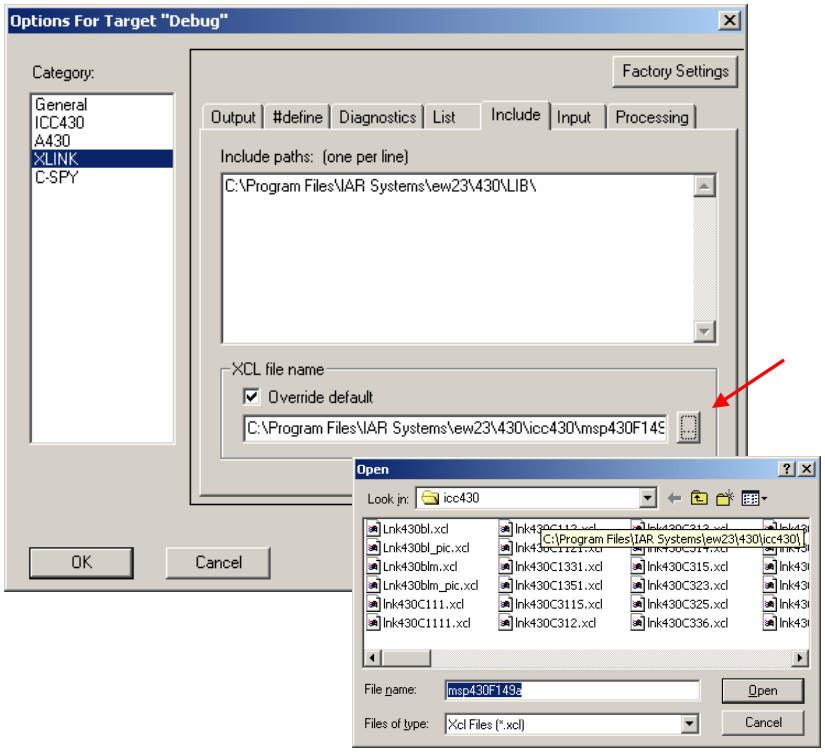

Figure 21. XLINK Submenu in the Options Menu.

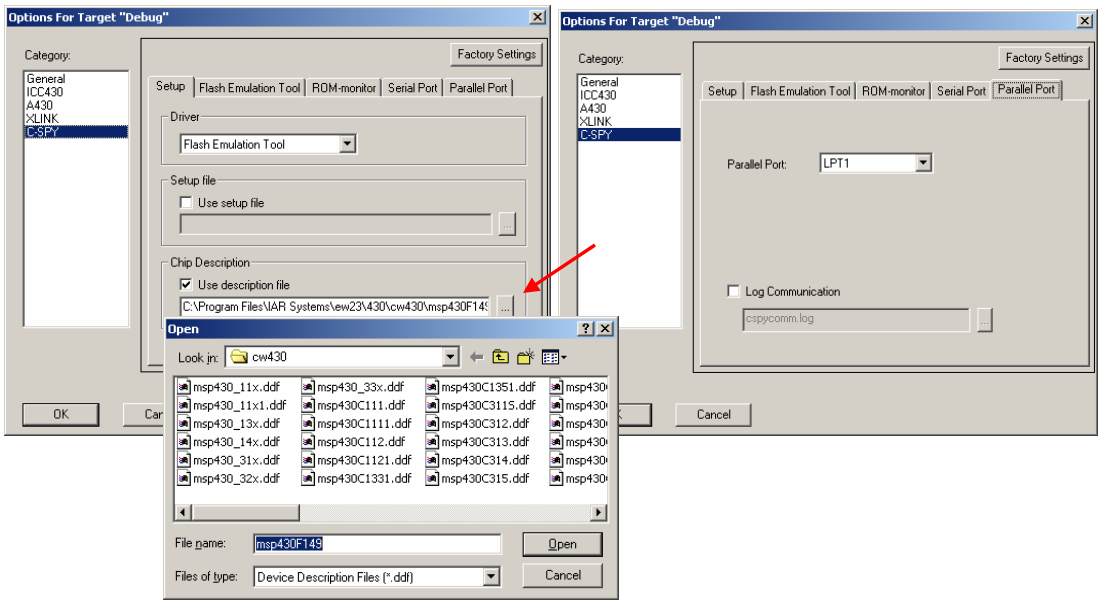

Figure 22. C-SPY Submenu in the Options Menu.

When all the necessary updates are done, the firmware is ready to be compiled, linked, executed and uploaded to the microcontroller. All of these actions can be performed by pressing the *Debugger* button, as indicated by the red arrow in Figure 23.

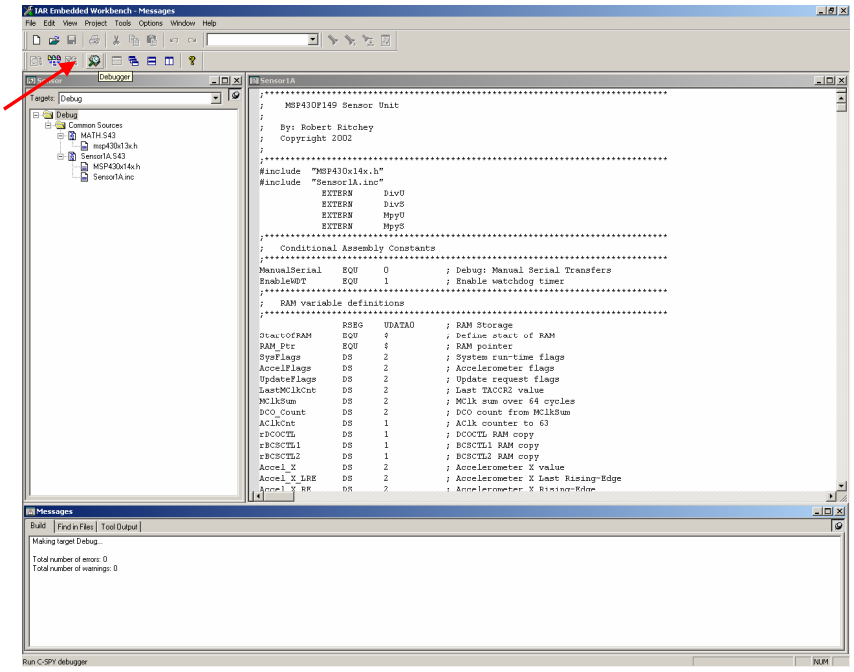

Figure 23. Debugging and Uploading the Firmware.

At this point the firmware uploading procedure is complete. The MARG sensors and the CIU are ready to use.

B. THE CALIBRATION PROCEDURE

The output of the MARG III sensor is nine voltages, which represent the nine different magnetic, gravity and angular rate measurements of the sensor's orientation and motion. Unfortunately, voltages are not meaningful to the filtering algorithm. Therefore, the data must be *transformed* into something meaningful, such as gravity (g), magnetic field (gauss) and angular rate (deg/s).

Furthermore, each micromachined sensor has its own characteristics. Therefore, identical micromachined sensors (e.g., two ADXL202E accelerometers) may produce slightly different outputs for the same orientation. Since the accuracy of the visual representation of the limb motion depends heavily on the accuracy of the measurements, the data *correction* should precede filtering.

In order to perform such *transformation* and *correction,* a calibration procedure is followed. The output of this procedure is three magnetometer and three accelerometer *null values*, and the corresponding *scaling factors* [Ref. 2]. As mentioned in an earlier chapter, the rate sensors were not taken into consideration for the purpose of this thesis.

The calibration procedure used in this thesis was an improved version of the one developed by Bachman [Ref. 2]. It consisted of sequential 90^{o} or 180^{o} rotations for the accelerometer and the rate sensor calibration, followed by three 360^{o} rotations about the west-east orientation for the magnetometer calibration.

In Bachman's original work [Ref. 2] and in a more recent publication [Ref. 9], it is stated that the calibration can be performed without using any specialized equipment, due to the linear characteristics of the micromachined components.

Nevertheless, extensive experiments indicate that the calibration by hand does not provide consistent null values and scaling factors for the magnetic sensors. Therefore, a more accurate procedure was chosen. This procedure involved the

same steps used for MARG II, but the sequential rotations regarding the magnetometer calibrations were performed with a HAAS tilting/rotating table, shown in Figure 24.

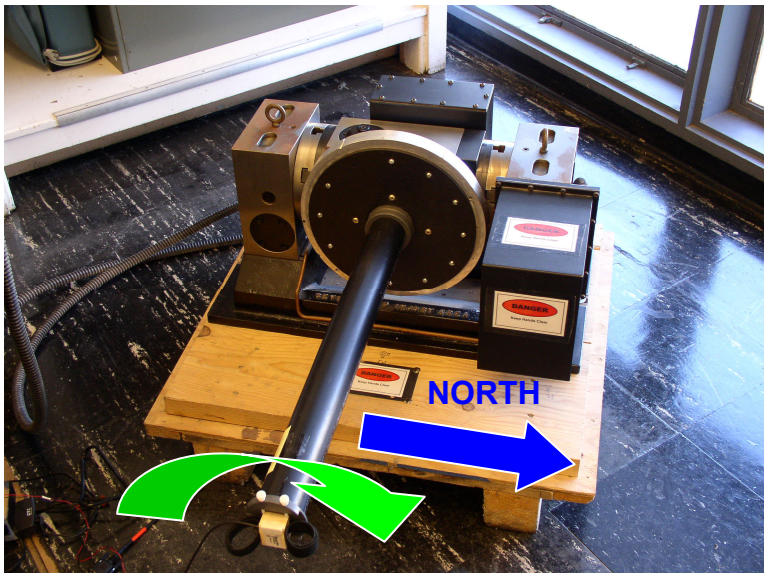

Figure 24. The HAAS Tilting/Rotating Table.

The software used to perform the calibration was an improved version of the same software used for the MARG II sensors. Changes had to be made to achieve communication between the CIU and the Data Reader Server, but other than that, the main calibrating algorithm was implemented as a 33-state machine [Ref. 2, pp. 115-121].

Briefly, the accelerometer calibration involved placing the sensor sequentially on a level surface with the positive *x*-axis first pointing up, and then pointing down. For each position, 100 measurements were taken and averaged. The same procedure was followed for the *y*- and *z*-axis accelerometers.

The magnetometer calibration made use of the HAAS table, which had to be placed on a level surface, with the orientation shown in Figure 24. For the calibration of the *x*-axis magnetometer, the sensor was placed with the positive *x*-axis pointing to the magnetic north (identified by a magnetic compass) and the *y*-

axis aligned to the east-west orientation. A rotation of 720^{o} was performed about the east-west axis, as shown by the green arrow in Figure 24. Similarly, for the calibration of the *y*-axis magnetometer, the sensor was placed with positive *y*-axis pointing north and *z*-axis aligned to the east-west orientation. Finally, for the calibration of the *z*-axis magnetometer, the positive *z*-axis was pointing north and the *x*-axis was aligned to the east-west orientation.

In addition to the *null values and scaling factors*, the *reference magnetic* and *gravity vectors* were computed for the following MARG III sensor orientation: the positive *z*-axis pointing north, the positive *y*-axis pointing up and the positive *x*-axis pointing west. The significance of the *reference vectors* is discussed in the next chapter, in which the QUEST algorithm is used to perform data filtering.

1. Validation of Calibration Results

After each sensor calibration, the accuracy of the procedure had to be verified. For that reason a MATLAB® code was created to read the sensor data and the calibrating values from a file. Then it calibrates the sensor data and displays the calibrated results.

In order to have a common basis for comparing the calibrating results and the overall behavior among the MARG III sensors, the following motion patterns were studied:

- *Pattern 1*: A 720^{o} rotation about the *z*-axis aligned to an east-west orientation and the *x*- and *y*-axes rotating on the north-south vertical plane, and
- *Pattern 2*: A 720^{o} rotation about the *x*-axis aligned to an east-west orientation and the *y*- and *z*-axes rotating on the north-south vertical plane.

From the above rotations, the following results were expected:

- For *Pattern 1*: The response of the *z*-axis magnetic and gravity sensor should be zero at all times or at least very close to zero. The *x*-

and *y*-axes magnetic and gravity sensors should provide perfect sinusoids fluctuating between minus one and plus one.

- For *Pattern 2*: The *x*-axis magnetic and gravity sensor should be zero at all times or at least very close to zero. Similarly, the *y*- and *z*-axes magnetic and gravity sensors should provide perfect sinusoids fluctuating between minus one and plus one.

The rotations were performed as positive right-handed rotations assuming west is the positive rotation axis.

2. Results – MARG III Sensor Redesign

The outcome of the calibration for a MARG III sensor is shown in Figure 25. The sensor followed *pattern 1* motion. Therefore the rotation was performed about the *z*-axis, with the positive *x*-axis originally pointing north and the positive *y*-axis pointing up. The solid lines represent the *raw* data gathered from the sensor, whereas the dashed lines represent the calibrated output.

As seen in the lower half of the figure, the *x*- and *z*-axis accelerometers values are initially zero, as indicated by the blue solid arrow. As the *x*-axis starts to tilt down, its gravity output starts to increase following a sinusoidal pattern. It reaches its maximum value (normalized at one) when the *x*-axis points vertically, away from the ground. Since the *y*-axis accelerometer was initially pointing up, the minimum value of minus one was expected (green arrow). As it starts to rotate toward the north (tilting toward the ground), its acceleration output value starts to increase.

It can be clearly seen that it reaches zero at the exact moment the *x*-axis accelerometer produces its maximum value. Finally, the *z*-axis accelerometer always produces zero values.

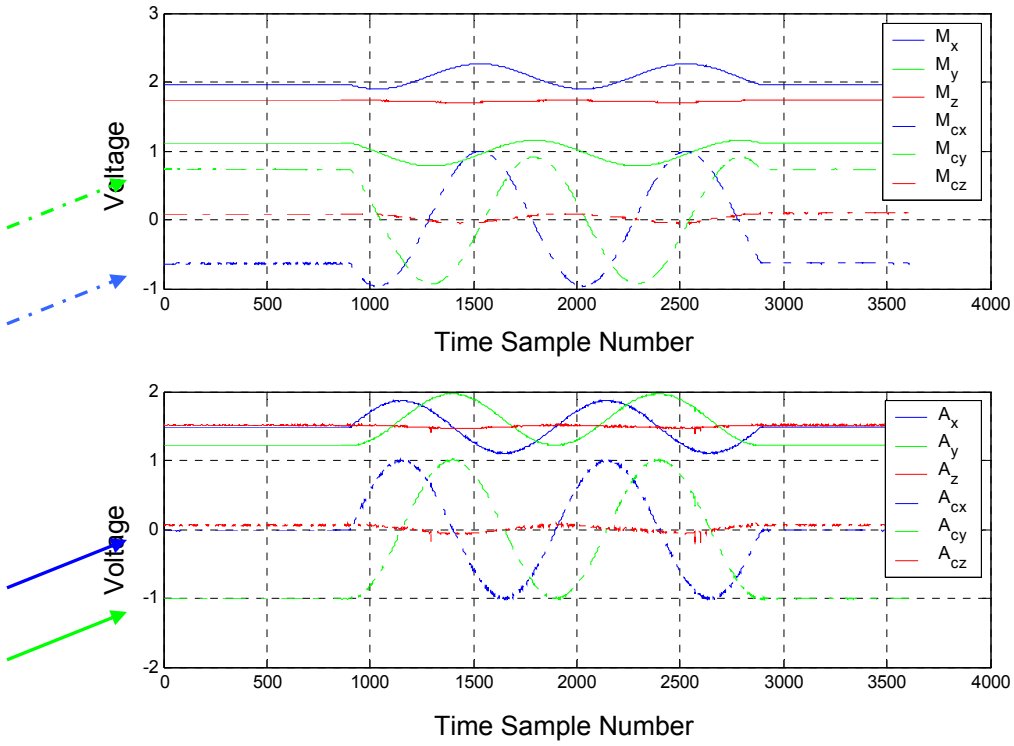

Figure 25. Calibration Results for *x*: North, *y*: Up, *z*: East, Rotation about *z*.

Before continuing with the magnetic sensor analysis, a brief discussion about the earth's magnetic field is in order. A magnetic sensor produces its maximum output when it is aligned to the magnetic lines of the earth's magnetic field. Depending on the latitude, the magnetic lines entering the earth's surface have a different angle, as shown in Figure 26.

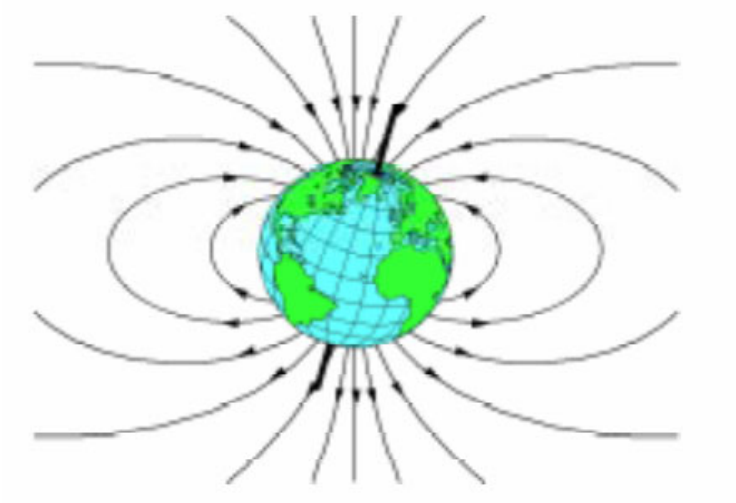

Figure 26. Earth's Magnetic Field Lines [From Ref. 18.].

This research took place in Monterey, California, where the latitude is 36.6°. This means that the magnetic lines enter the ground at an angle of approximately 60°. Therefore, the maximum magnetic value should be taken from a sensor pointing toward the magnetic north (as indicated by a magnetic compass) when the sensor is tilted to the ground at an angle of approximate 60° from the horizontal level.

As seen in the upper half of Figure 25 (indicated by the blue dotted arrow), the x-axis magnetic sensor produces a negative value, even though the sensor points to the north. As the sensor begins to tilt toward the ground, the magnetic value decreases more and reaches its minimum value (instead of the maximum) when the sensor points almost at 60° down. The same inconsistent result is observed for the y-axis magnetometer (green dotted arrow).

Further testing following *pattern 2* showed the same response from the *z*-axis magnetic sensor. Therefore, even though the sensors seemed to be calibrated, they produced the opposite sense for the rotations.

The above results meant that the MARG III design, concerning the Honeywell magnetic sensors, needed to be reviewed closely.

Further investigation showed that the design sheet that Honeywell provided for the magnetometer HMC1051Z had an erratum that indicated a reversed polarity on the set-reset strap of the sensor. After contacting Honeywell technical support, the erratum was confirmed [Ref. 19]. Consequently, the sensor wired as shown on the design sheet showed a maximum magnetic field when pointing south. This anomaly had been observed during the initial construction of the MARG III sensor. Therefore, the set-reset straps of the *x*- and *y*-axis magnetic sensor were wired with reverse polarity to achieve uniformity between the outputs of all three magnetometers. This resulted in all three magnetometers always showing reversed magnetic fields.

By rewiring the sensors and by making a slight change to the firmware uploaded to all the MARGIII sensors regarding the set-reset polarity, the problem was solved and the calibration results behaved as expected.

Since the accelerometers are designed to measure combined static (gravity) and dynamic accelerations, and since the rotations were performed at a relatively slow rate of 36 deg/sec, a second consideration was made about the accelerometer output. According to the calibration technique, the accelerometers should provide maximum and minimum values of positive and negative 1 g when pointing down and up, respectively. Since the accelerometers can measure within the range of ± 2 g, the maximum static accelerations should be only half of the maximum value. Therefore, the possibility of dividing the accelerometer scaling factors provided by the calibration sequence by a factor of 2 was considered. The reason was to minimize the possibility of saturating the accelerometers when sustaining the combined static and dynamic accelerations.

The results from a calibrated rotation about the *x*-axis, when the positive *y*-axis was initially pointing down and the positive *z*-axis was pointing north, is shown in Figure 27. All the calibrated data behave as expected.

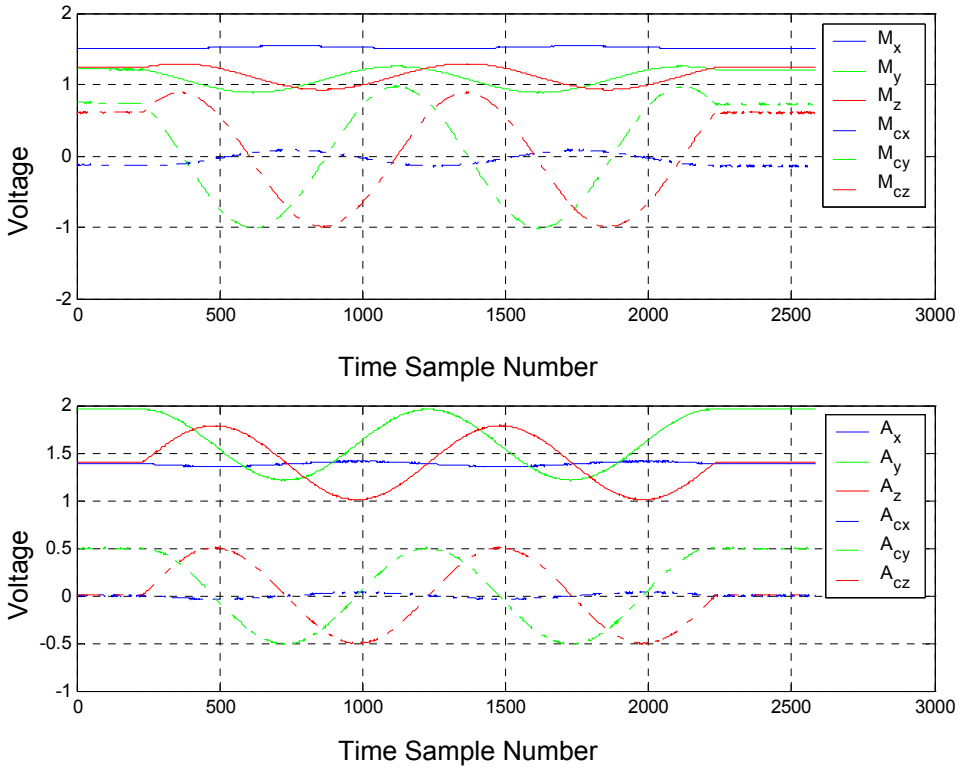

Figure 27. Calibration Results for *x*: East, *y*: Down, *z*: North, Rotation about *x*.

C. SUMMARY

This chapter presented the firmware uploading procedure and the MARG III sensor calibration. The test results that led to the MARG III being redesigned were also discussed. In the following chapter, the effort of testing the CIU is examined. The QUEST algorithm as a quaternion filter is also discussed.

THIS PAGE INTENTIONALLY LEFT BLANK

V. VISUALIZATION OF THE MARG III SENSOR DATA

This chapter describes the process for visualizing the MARG III data delivered by the CIU. The QUEST algorithm was selected to filter the data. Some modifications were introduced to increase the accuracy of the algorithm results. MATLAB® and SIMULINK® simulations are performed in order to validate the response of the sensors. Finally, this chapter also presents the combined efforts of this research and the research of another thesis [Ref. 3] to implement an X3D based human avatar.

A. THE QUEST ALGORITHM

Filtering the calibrated data requires a computationally efficient algorithm, capable of tracking limb motion without any singularities. For this reason, the QUEST algorithm was chosen [Ref. 20]. This algorithm was created to determine the attitude of a rigid body in reference to a fixed coordinate system, using a set of measurement vectors. The goal of the algorithm was to compute a *rotation (attitude) matrix A,* capable of rotating the measurement vectors (assuming no errors introduced) so as to match exactly the reference vectors. *Matrix A* has nine elements, which have proven to be difficult to determine [Ref. 20]. Therefore, the QUEST algorithm was designed to compute a *quaternion* that describes attitude with four elements. Once the *quaternion* was computed, the *rotation matrix A* could be determined, and vice versa. The QUEST algorithm has been successfully used in the past in various applications (e.g., satellite tracking, etc.) [Ref. 20].

The MARG III sensor produces three measurement vectors every one hundredth of a second. The magnetic vector consists of the magnetic field components measured in the three directions *x*, *y*, and *z*. Similarly, the angular rate vector holds the *x*, *y*, and *z* components of the angular rate measurements. Finally, the gravity vector measures the three components of the earth's gravity field. The minimum number of attitude measurement vectors required by the

QUEST algorithm to produce an output is two. The magnetic field and the gravity vectors produced by the MARG III sensor are related to attitude. The third vector measures rate and therefore cannot be used as an input for the QUEST algorithm.

In the previous chapter, the need to acquire a set of reference vectors during the calibration procedure was mentioned. When studying a single rigid body, the set of these vectors can be chosen arbitrarily. On the other hand, when studying multiple limbs linked to each other, the choice of the set of reference vectors cannot be arbitrary. In this case, the reference vector sets should coincide for all the associated limbs. Therefore, the magnetic field and gravity reference vectors should be defined with all the MARG III sensors having the same orientation.

The algorithm requires the computation of eigenvalues of a specific matrix *K* as discussed later. At the time the QUEST algorithm was first introduced in 1981, computers were not as powerful as today. For computational efficiency, the algorithm was designed based on the acceptance that unit reference vectors and measurements produce eigenvalues very close to one. The need for precise computation of the eigenvalues was avoided at the expense of less accurate quaternions. Today, computational power is not an issue. Therefore, in order to improve the accuracy of the algorithm, the eigenvalues are computed precisely.

B. MATLAB® AND SIMULINK® SIMULATIONS

As expected, the sensor measurements are contaminated by noise. Therefore, simulations had to be done in order to evaluate the performance of the system. For this reason, the SIMULINK® model shown in Figure 28 was created.

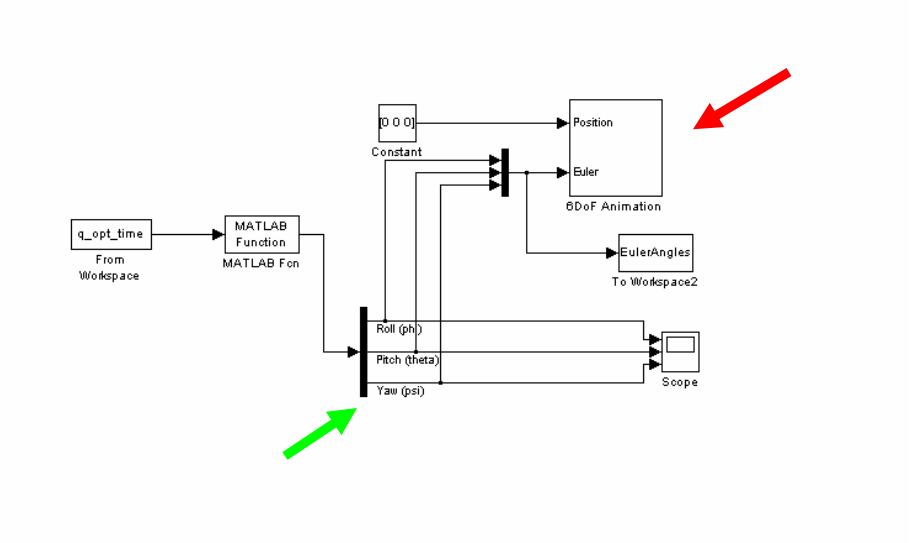

Figure 28. The SIMULINK® Model Created to Visualize the Results.

With the use of MATLAB®, the necessary functions were created by the author to implement the QUEST algorithm. The algorithm was implemented as shown in Figure 29.

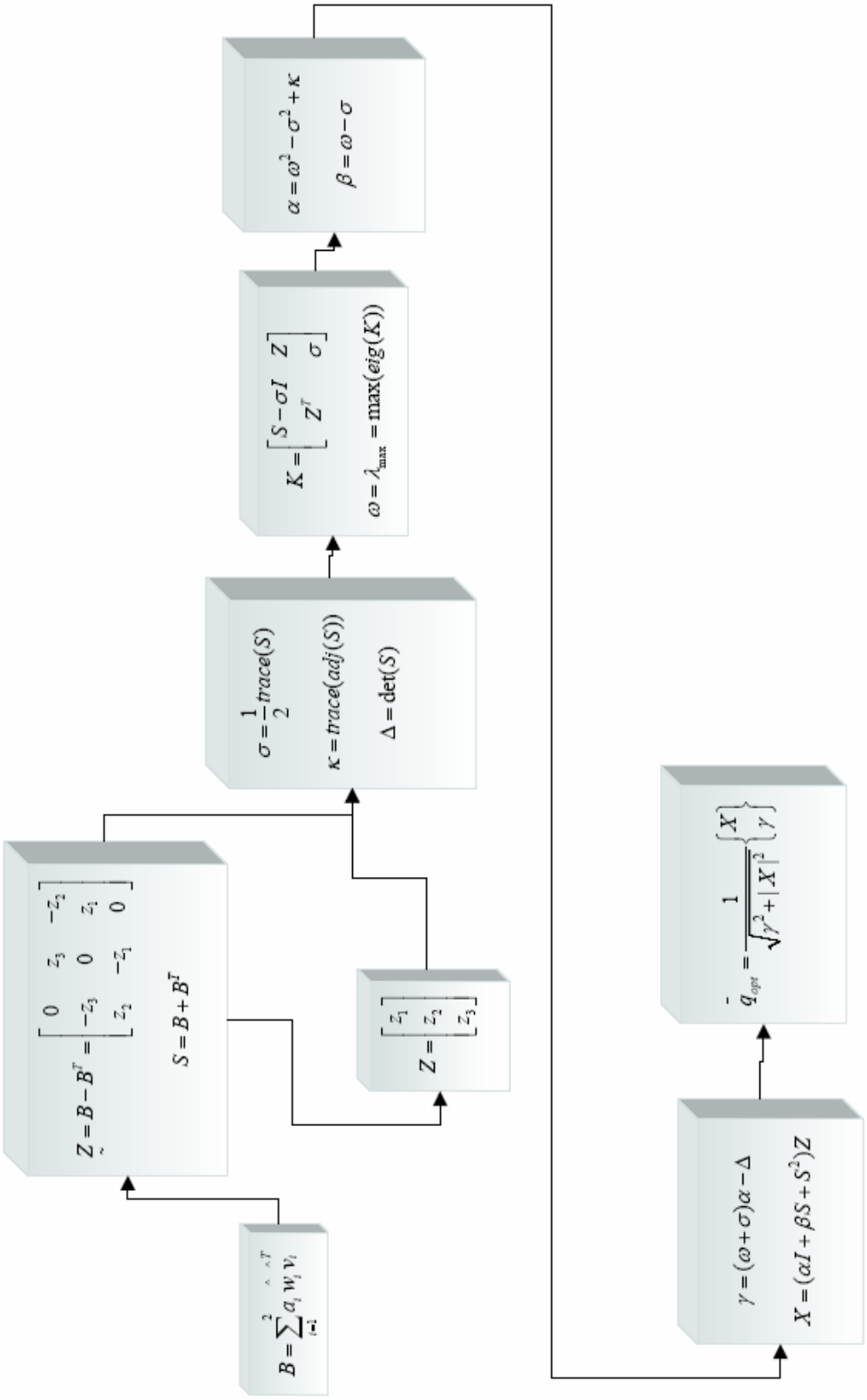

Figure 29. The Block Diagram of the QUEST Algorithm

The MATLAB® code is available upon request from Professor Xiaoping Yun (yun@nps.navy.mil).

In the first block of the above figure, a *B* matrix is computed from the reference vectors v_1 and v_2, the measurement vectors w_1 and w_2 and the weighting vector α. The weighting vector is chosen to weight the importance of the measurement vectors, and its norm is equal to one. For the MARG III sensor, w_1 and w_2 are the acceleration and magnetic measurements. The *B* matrix is used to compute the 3 x 3 matrix *S* and the 3 x 1 vector *Z.* Then the scalars σ, κ, Δ are computed as shown in the above figure. Finally, the 4 x 4 matrix *K* is constructed and its maximum eigenvalue is computed before calculating the scalars α, β, γ and the 3 x 1 vector *X*. The vector *X* and the scalar γ together provide the optimum quaternion that describes the attitude of the MARG III sensor.

Data from the MARG III sensors were captured and fed to the algorithm. The sensors were performing rotations according to the two *patterns*, mentioned in the previous chapter. The calibration data were loaded as MATLAB® files.

As seen in Figure 28, the computed quaternions were transformed into *Euler angles* (roll φ, pitch θ and yaw ψ, indicated with the green arrow). To visualize the motion captured by the MARG III sensors, a 6 degree-of-freedom (DOF) missile provided by SIMULINK® was used (red arrow in Figure 28), as shown in Figure 30.

The results showed that the algorithm responded well. The missile followed the patterned rotations very closely. The Euler angles for a rotation following *pattern 2* are presented in Figure 31.

The missile was expected to perform a 720^o rotation (roll φ) about its longitudinal axis. No pitch or yaw motions were expected to appear. The corresponding motion of the missile was an exact 720^o rotation about *x*-axis. Figure 31 shows that the missile starts with a zero roll. When the motion starts, the missile responds with a linear rotation toward negative 180^o. The system measures angles within the range of negative 180^o and positive 180^o. Therefore, a sudden

transition from negative 180^{o} to positive 180^{o} appears in Figure 31. In reality, the missile continuous to rotate with a constant angular rate until it performs a full 720^{o} rotation and then it stops. A slight pitch deviation and an even smaller yaw deviation, possibly due to imperfections in the calibration, are also noticed in Figure 31.

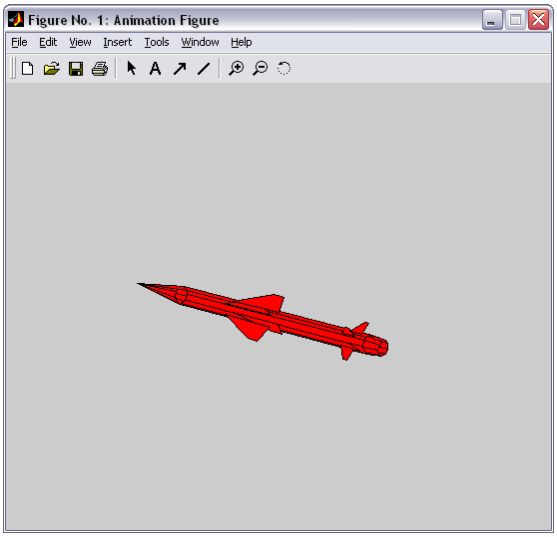

Figure 30. The SIMULINK® Rigid Body Missile.

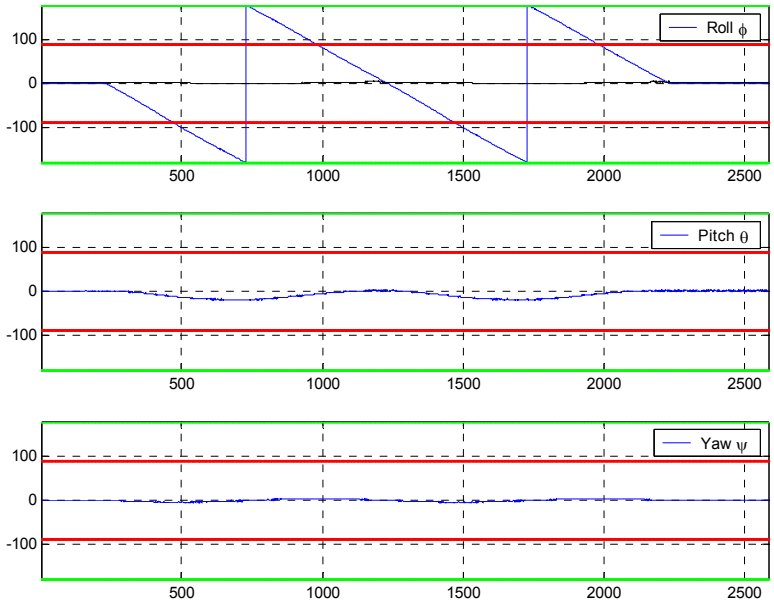

Figure 31. Euler Angles for a *Pattern 2* Motion.

C. REAL-TIME VISUALIZATION OF THE SENSOR DATA

Since the MATLAB® simulation results were satisfactory, real-time testing was performed next. Another thesis focusing on the development of an X3D avatar [Ref. 3] was conducted simultaneously. In that effort the QUEST algorithm was implemented in JAVA along with server-client programs capable of acquiring the MARG III data of this thesis from the CIU in real time. Wireless IEEE 802.11b communication was established in an effort to detach the tracked body from the rest of the hardware involved.

After the calibration, the sensor data were filtered, and the resulting optimal quaternions were transformed into axis-angle pairs by a client program. This transformation was necessary since the avatar was created in VRML language (X3D Graphics Specification), which has been standardized to use axis-angle pairs to represent rotations [Ref. 21].

The avatar was created in two stages. First, a human left arm was designed as shown in Figure 32. After all the tests were performed successfully with the one-arm avatar, the whole human body was introduced. The final version of the human avatar is shown in Figure 33.

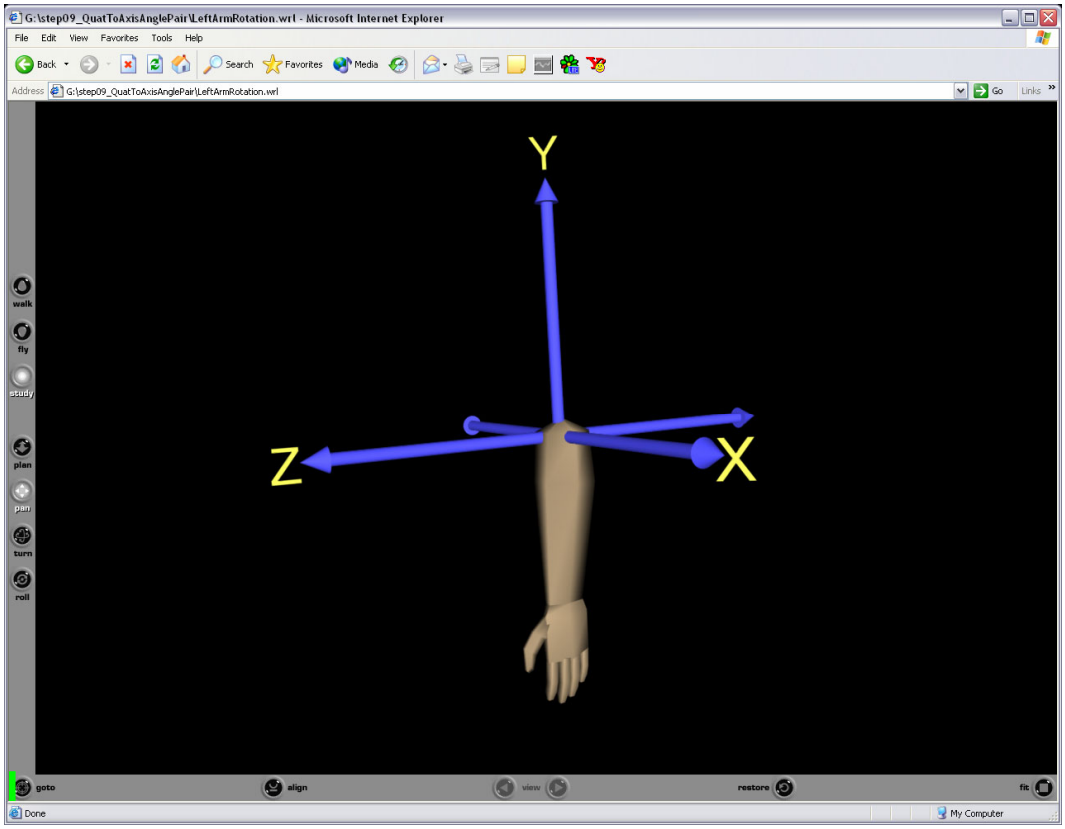

Figure 32. Left Lower Arm Avatar Created in X3D Format.

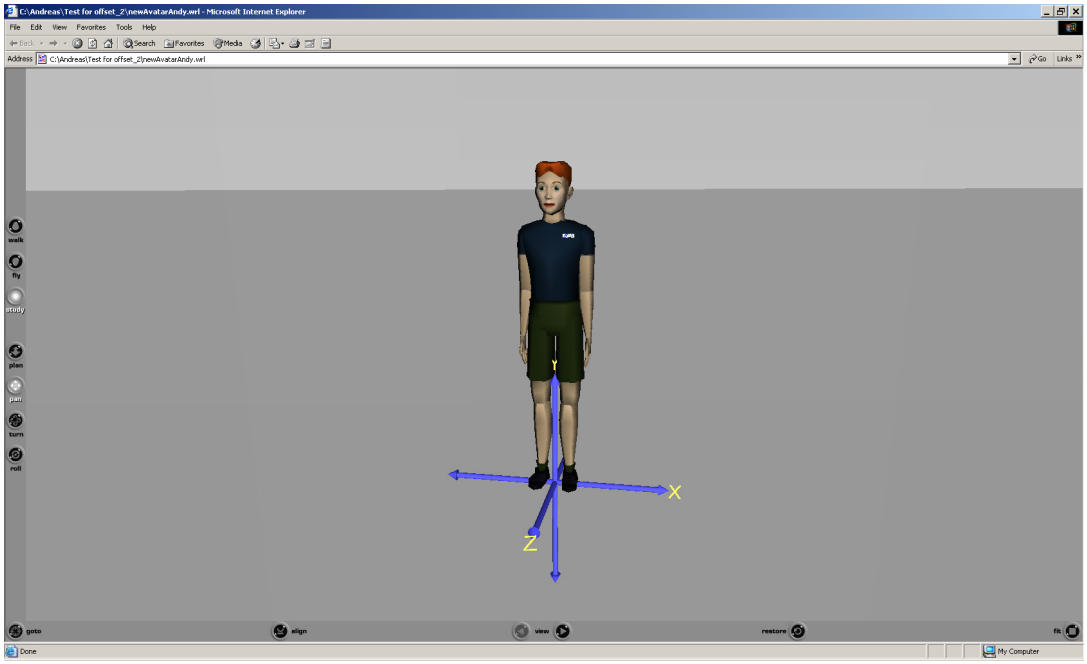

Figure 33. The X3D Human Avatar.

When the avatar is in a *resting* position, all the limbs are initially aligned with a coordinate system as shown in Figure 33. It can be seen that the *z*-axis extends from the front of the body, the *y*-axis is pointing up and the *x*-axis is pointing to the left of the avatar.

The MARG III sensors measure the attitude of the limbs in reference to a fixed coordinate system, as mentioned earlier in this chapter. In order to achieve coincidence between the attitude measured by the sensors and the one represented by the human avatar, these reference vectors should be captured with the sensors oriented identically to the avatar. This means that the sensor's *z*-axis must be parallel to the ground, and the positive *y*-axis should be vertical to the ground and facing up. The *x*-axis should be placed consequently. As long as this constraint holds, it does not matter what the azimuthal orientation of the MARG III sensors is at the starting position, since the avatar has relative *azimuthal feeling* only, and not absolute. Therefore, if all sensors have their positive *z*-axis oriented to a constant point on the horizon (e.g., north), the reference vectors captured will coincide with the avatar's coordinate system. For the purposes of this thesis, the reference azimuthal orientation was chosen to be with the positive *z*-axis pointing to magnetic north, as described in Chapter IV.

The testing results with the full-body avatar were very successful. With the use of two MARG III sensors, the avatar followed the motion of the human right arm exactly. Figure 34 and Figure 35 show snapshots, in which the user has two MARG III sensors attached to his right arm. The user moves his arm, and the motion is followed in real time by the avatar. If a fast motion is performed, the system loses the accuracy during the transition. This occurs because fast motions introduce high dynamic accelerations that *contaminate* the gravity field measurements. Furthermore, when the accelerometers exceed their maximum measurement range (± 2 g), they saturate, and the QUEST algorithm produces inaccurate quaternions. Nevertheless, when the arm reaches its final position, the system resumes its accuracy, and the represented limb attitude becomes precise (steady-state response).

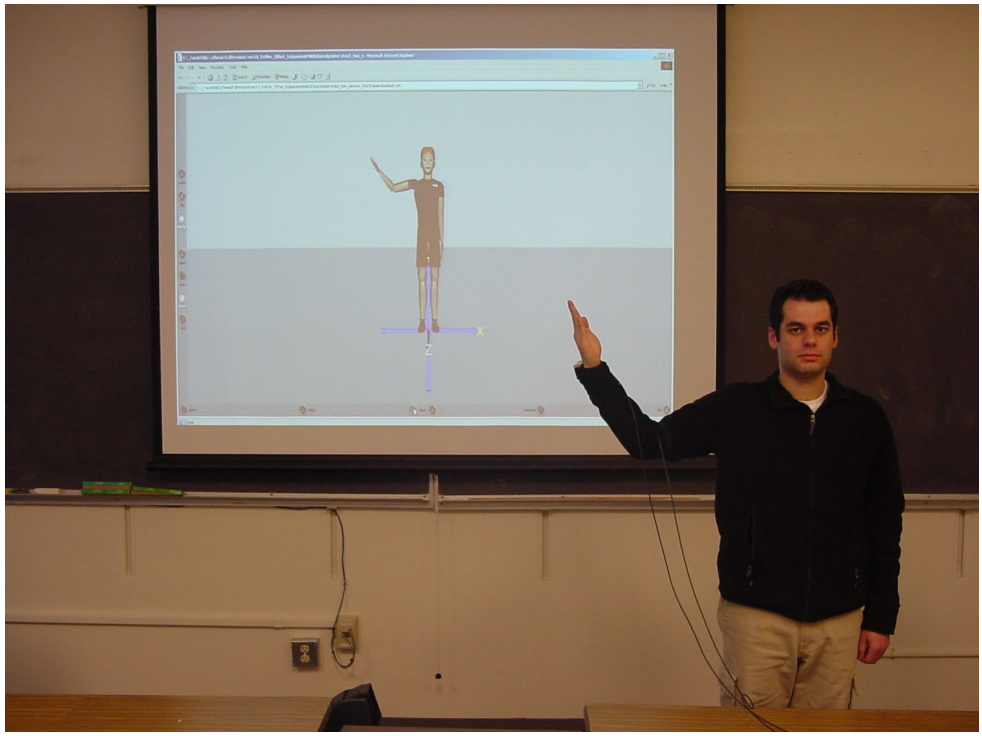

Figure 34. Real-time Projection of a Human Arm Motion Using Two MARG III Sensors.

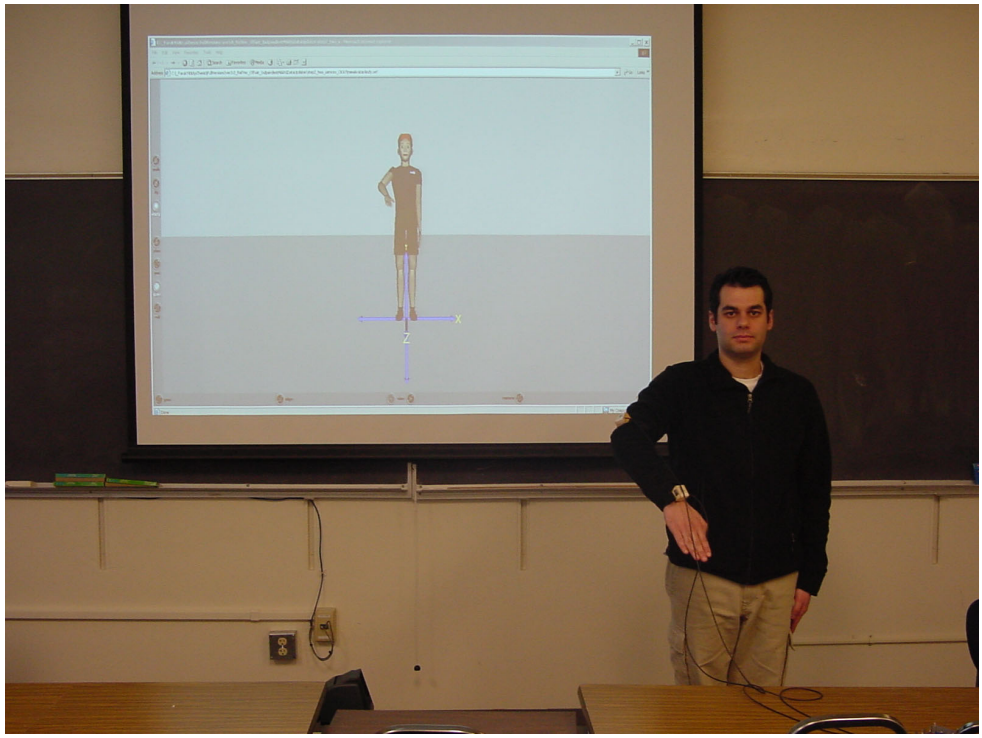

Figure 35. Real-time Projection of a Human Arm Motion Using Two MARG III Sensors.

When the rate sensor measurements are combined with the QUEST algorithm using a Kalman filter, the system performance is expected to improve during the transition motions [Ref. 22].

D. SUMMARY

The efforts to verify the functionality of the MARG III sensor and the CIU were discussed in this chapter. The QUEST algorithm was chosen to filter the data delivered by the CIU. Visual representation was first achieved by using a SIMULINK® model. Finally, combined efforts of this research and the research of another thesis [Ref. 3] led to the design of an X3D human avatar visualizing the motion of a tracked human body in real time.

THIS PAGE INTENTIONALLY LEFT BLANK

VI. CONCLUSIONS AND FURTHER WORK

A. THESIS CONTRIBUTIONS

This thesis has developed a system for tracking the motion of a human body by the use of the MARG III sensors. The system uses data provided by the sensors to achieve the *immersion* into a *Virtual Environment*.

The main components of the system, other than the MARG III sensors, are the Control Interface Unit (CUI), the Wiser 2400 serial-to-wireless transmitter, and a server capable of filtering the data delivered by the CIU. Clients can connect to the server at any time and provide a real-time visual representation of the human motion.

The digital data from the MARG III sensors are parsed into 12-bit words and are transmitted through an SPI connection to the CIU. The CIU sends the data through an RS-232 connection to the serial-to-wireless transmitter. Then, the data are filtered and transformed into quaternions with the use of the QUEST algorithm. Finally, the quaternions are converted into axis-angle pairs, which are used by an X3D human avatar designed to project the 3-DOF motion of a human body on a computer screen.

The heart of this system and the main component studied in this thesis is the CIU. At this moment, it is capable of receiving data from three MARG III sensors and of preparing them to be transmitted wirelessly through Wiser 2400 transmitters at a speed of 19.2 kbps for each MARG III sensor. The CIU is also capable of providing the MARG III sensors with the necessary power to operate, and it also synchronizes the SPI communication by providing the clock. It was developed in two stages. The first stage involved the design and implementation of a one-channel CIU facilitating the testing and evaluating of a single MARG III sensor. Then the three-channel CIU (three one-channel CIUs in a parallel configuration), capable of transmitting data from three MARG III sensors, was implemented and tested successfully.

The QUEST algorithm is used to filter the measurement data. It represents the human body motion in the form of quaternions. It uses the accelerometer and magnetometer measurements provided by the MARG III sensor to compute the attitude of the rigid body in reference to a constant set of vectors with no singularities. The QUEST algorithm is also very efficient for low frequency motions but quite inaccurate for fast moving limbs.

Finally, the MARG III sensor is designed to be small and energy efficient due to the characteristics of its components. It provides real-time tracking measurements sampled at a rate of 100 Hz, which has proven to be sufficient. The measurements are provided by three magnetometers, three accelerometers and three rate sensors in the MARG III sensor forming an orthogonal triad.

B. FURTHER DEVELOPMENT

The three-channel CIU is capable of transmitting data from three MARG III sensors without performing any multiplexing. Each MARG III sensor has its data transmitted wirelessly to the server through an independent thread. This involves using three different Wiser 2400 transmitters. To overcome the problem of using multiple transmitters, the sixteen-channel CIU was designed. At the time of this writing, it is approaching its final steps of development. The new CIU will be capable of receiving data from sixteen sensors simultaneously with a sampling rate of 100 Hz, multiplexing them, and transmitting them through a wireless connection. Issues involving the high data-transmission rate of 232 kbps needed to achieve transmission from all the MARG III sensors (including the overhead) will have to be solved.

A complementary filter is needed to supplement the existing QUEST algorithm. The new filter should receive the quaternions produced by the QUEST algorithm and filter them along with the measurements delivered from the rate sensors. Issues involving the bias introduced by the accelerometers from measuring the combination of dynamic and static accelerations must be solved (by low-pass

filtering). *Drifting* of the output, introduced by the inability of the rate sensors to track low frequencies (slow motion) accurately, must be removed (high-pass filtering).

As technology evolves, the MARG sensor can be upgraded. The next generation of MARG sensors, called the MARG IV, is currently under development. With even smaller components, it is expected that the future design of MARG sensors could even be sewed on fabric.

The current system tracks a slow moving human body accurately. All the experimental results have indicated that after the development of the sixteen-channel CIU and the complementary filter, the system will be capable of tracking fifteen human limbs accurately. Visual representation and thus *immersion* into the Virtual Environment can be achieved without any of the limitations that the MARG II sensors introduced. The 100-Hz sampling rate has proved sufficient for real-time tracking of a human body motion. Implementing the system for *immersion* of more than one user into the same Virtual Environment is possible.

THIS PAGE INTENTIONALLY LEFT BLANK

LIST OF REFERENCES

1. Synthetic Environment Laboratory, *Synthetic Environments,* [http://www.sel.bee.qut.edu.au/understand/understand.htm], last accessed January 2004.

2. Eric R. Bachmann, "Inertial and Magnetic Tracking of Limb Segment Orientation for Inserting Humans into Synthetic Environments," Ph.D. Dissertation, Naval Postgraduate School, Monterey, CA, December 2000.

3. Faruk Yildiz, "Implementation of Human Avatars for the MARG Project in Networked Virtual Environments," MS Thesis, Naval Postgraduate School, Monterey, CA, March 2004.

4. J. Bers, "A Model Server for Human Motion Capture and Representation," *Presence: Teleoperators and Virtual Environments*, Vol. 5, No. 4, MIT Press, Cambridge MA, pp. 381-392, Fall 1996.

5. Honeywell Inc., *Honeywell 1, 2, and 3-axis Magnetic Sensors, HMC1051 / HMC1052 / HMC1053*, October 2003, Rev. -, [http://www.ssec.honeywell.com/magnetic/datasheets/HMC105X.pdf], last accessed February 2004.

6. Analog Devices Inc., *Analog Devices ADXL202E Low-Cost ± 2 g Dual-Axis Accelerometer with Duty Cycle Output,* 2000, Rev. A, [http://www.analog.com/UploadedFiles/Data_Sheets/567227477ADXL202E_a.pdf], last accessed February 2004.

7. Analog Devices Inc., *Analog Devices ADXL202E image,* [http://www.analog.com/productSelection/images/ADXL202E_cerpak_vs_penny.jpg], last accessed February 2004.

8. NEC TOKIN Corporation, *NEC TOKIN Sensors,* September 2000, Vol. 03, Rev. 2003, pp. 23-24, [http://www.nec-tokin.com/english/product/pdf_dl/sensors.pdf], last accessed February 2004.

9. Eric R. Bachmann, Xiaoping Yun, Doug McKinney, Robert B. McGhee, and Michael J. Zyda, “Design and Implementation of MARG Sensors for 3-DOF Orientation Measurement of Rigid Bodies,” *Proceedings of the 2003 IEEE International Conference on Robotics and Automation (ICRA 2003)*, Taipei, Taiwan, pp. 1171-1178, September 14–19, 2003.

10. Texas Instruments Incorporated, *MSP430F149 Product Information,*1995-2003, [http://focus.ti.com/docs/prod/folders/print/msp430f149.html], last accessed January 2004.

11. Texas Instruments Incorporated, *Texas Instruments MSP430x13x, MSP430x14x, MSP430x14x1 Mixed Signal Microcontroller Datasheet*, July 2000, Rev E, August 2003, [http://focus.ti.com/lit/ds/symlink/msp430f149.pdf], last accessed January 2004.

12. OTC Wireless Inc, *WiSER 2400 802.11b Wireless Serial Port Adapter User Guider,* Version 1.01, 2001, [http://www.otcwireless.com/support/downloads/wiser/Wiser9600/WiSER2400UG.pdf], last accessed February 2004.

13. MAXIM Integrated Products, *MAX3238* +3.0V to +5.5V, 1µA, up to 250kbps, True RS-232 Transceiver with AutoShutdown Plus,* Rev 1, 10/02, [http://pdfserv.maxim-ic.com/en/ds/MAX3238.pdf], last accessed February 2004.

14. Doug McKinney, *MARG III Command and Control Diagram,* Rev. B, McKinney Technology, Chandler, AZ, 08 December 2003.

15. XILINX Inc., *Spartan-II 2.5V FPGA Family: Complete Data Sheet,*3 September 2003, [http://www.xilinx.com/bvdocs/publications/ds001.pdf], last accessed February 2004.

16. *Webopedia Online Encyclopedia,* [http://www.webopedia.com/TERM/A/ASIC.html], last accessed February 2004.

17. Sander Electronic, *Starterkits für MSP430-Controller: MSP-FET-430,* October 2003, [http://www.sander-electronic.de/es0004.html], last accessed February 2004.

18. Michael J. Caruso, *Applications of Magnetoresistive Sensors in Navigation Systems*, Honeywell Inc., February 1998, [http://www.ssec.honeywell.com/magnetic/datasheets/sae.pdf], last accessed February 2004.

19. Doug McKinney in email communication, McKinney Technology, Chandler, AZ, 14 November 2003.

20. M. D. Schuster and S.D. Oh, “Three-Axis Attitude Determination from Vector Observations,” *Journal of Guidance and Control,* Vol. 4, No. 1, pp. 70-77, January-February, 1981.

21. Andreas Jochheim, Michael Gerke, and Andreas Bischoff, *Modeling and Simulation of Robotic Systems*, *Frame Transformations in VRML,* Control Systems Engineering group, Department of Electrical Engineering, University of Hagen, Version 3.0, 17 August 200, [http://icosym-nt.cvut.cz/odl/partners/fuh/course_main/node36.html,] last accessed February 2004.

22. Xiaoping Yun, Mariano Lizarraga, Eric R. Bachmann and Robert B. McGhee, "An Improved Quaternion-Based Kalman Filter for Real-Time Tracking of Rigid Body Orientations,” *Proceedings of Intelligent Robots and Systems*, Las Vegas, NV, pp. 1074-1079, October 2003.

THIS PAGE INTENTIONALLY LEFT BLANK

INITIAL DISTRIBUTION LIST

1. Defense Technical Information Center
   Ft. Belvoir, Virginia

2. Dudley Knox Library
   Naval Postgraduate School
   Monterey, California

3. Chairman Code EC
   Department of Electrical and Computer Engineering
   Naval Postgraduate School
   Monterey, California

4. Chairman Code IS
   Department of Information Science
   Naval Postgraduate School
   Monterey, California

5. Professor Xiaoping Yun, Code EC/Yx
   Department of Electrical and Computer Engineering
   Naval Postgraduate School
   Monterey, California

6. Professor David C. Jenn, Code EC/Jn
   Department of Electrical and Computer Engineering
   Monterey, California

7. Professor Eric R. Bachmann
   Department of Computer Science and System Analysis
   Miami University
   Oxford, Ohio

8. Professor Robert B. McGhee
   Department of Computer Science, Code CS/Mz
   Monterey, California

9. Doug McKinney
   President McKinney Technology
   Chandler, Arizona

10. Andreas Kavousanos-Kavousanakis
Athens, Greece

11. Faruk Yildiz
Gazipasa/Antalya
Turkey